Bol. Soc. Paran. Mat.
©SPM – E-ISSN-2175-1188
SPM: www.spm.uem.br/bspm

(3s.) **v. 2025 (43)** : 1–28.
ISSN-0037-8712
doi:10.5269/bspm.75875

Analysis of Fractional Order Mathematical Model of HIV-TB Using Atangana—Baleanu-Caputo Operator in the Presence of Treatment for TB

Agbata Benedict Celestine, Raimonda Dervishi, Erjola Cenaj, Habeeb A. Aal-Rkhais, Marcos Salvatierra, Shyamsunder, Bolarinwa Bolaji

ABSTRACT: This study presents a mathematical investigation of the transmission dynamics of HIV - Tuberculosis (TB) co-infection using the Atangana-Baleanu-Caputo (ABC) fractional operator with Mittag-Leffler kernel, representing a significant advancement over conventional integer-order models by capturing the memory-dependent nature of disease progression that traditional approaches cannot adequately represent. The model's mathematical rigor was established through existence and uniqueness analysis using the Picard-Lindelöf theorem, ensuring solution reliability. Comprehensive sensitivity and uncertainty analyses, with the basic reproduction number as the response function, identified three critical parameters driving TB transmission: the TB transmission rate, modification parameters for TB-only individual infectiousness, and latent TB treatment rates. Numerical simulations demonstrated that prioritizing treatment for individuals with latent TB infections—both TB-only and HIV-TB co-infected cases—significantly reduces both TB and HIV incidence rates in the population. The fractional-order framework successfully captures nuanced co-infection dynamics that conventional models miss, while our intervention analysis reveals that targeted treatment of latent TB infections represents a highly effective strategy for controlling the dual HIV-TB epidemic, providing evidence-based guidance for integrated healthcare policies.

Key Words: Atangana-Baleanu-Caputo derivative, HIV-TB co-infection, Existence and uniqueness, Sensitivity analysis, Numerical simulations.

Contents

Submitted February 25, 2025. Published September 01, 2025
2010 *Mathematics Subject Classification:* 34A08, 92D30, 33E12, 34A12.

1. Introduction

Human Immunodeficiency Virus (HIV) is a chronic viral infection that targets the immune system, particularly CD4 T-cells, leading to immune deficiency. If untreated, HIV progresses to Acquired Immunodeficiency Syndrome (AIDS), a condition characterized by severe immune suppression and vulnerability to opportunistic infections and cancers [1,4]. Globally, HIV remains a significant health challenge, with an estimated 39.9 million people living with the virus in 2023. Of these, about 9.3 million are not receiving antiretroviral therapy (ART), which is essential for managing the disease and preventing progression [4]. Efforts to combat HIV have made substantial progress, with ART expanding access and enabling people to live longer and healthier lives. For instance, ART coverage increased from 47% in 2010 to over 75% in 2023, a public health milestone [1,4]. However, stigma, discrimination, and disparities in healthcare access continue to hinder efforts, particularly in low- and middle-income countries. These barriers deter individuals from seeking testing and treatment, compounding the global burden of the epidemic [3]. Despite challenges, the global commitment to end AIDS as a public health threat by 2030 remains strong. Advocacy for human rights, education, and increased funding are pivotal to achieving this goal. Innovative approaches, including pre-exposure prophylaxis (PrEP) and community-based care models, have shown promise in preventing new infections and improving the quality of life for those living with HIV [4, 5].

Tuberculosis (TB), caused by Mycobacterium tuberculosis, is a communicable disease that primarily affects the lungs but can also disseminate to other parts of the body. It is transmitted through airborne particles, making it highly contagious. In 2022, TB caused 1.6 million deaths globally, with over 10.6 million new cases reported, marking an increase from previous years [2, 5]. This resurgence is partly attributed to the disruption of healthcare services during the COVID-19 pandemic, which reversed years of progress in TB control. Despite being preventable and curable, TB remains a major public health concern due to drug resistance, diagnostic delays, and treatment interruptions. The rise of multidrug-resistant TB (MDR-TB) poses a significant challenge, with only 60% of MDR-TB cases successfully treated in 2021 [5]. Advancements in diagnostics, such as GeneXpert, and shorter treatment regimens for drug-resistant TB have shown promise in improving outcomes, but access remains limited in resource-constrained settings [2,3]. The End TB Strategy, spearheaded by the World Health Organization, aims to reduce TB deaths by 90% and new cases by 80% by 2030. This ambitious goal requires addressing social determinants of health, enhancing healthcare infrastructure, and increasing funding for research and development of new vaccines and treatments [5]. Collaborative global efforts are essential to overcoming these barriers and eliminating TB as a public health threat.

HIV and TB frequently co-infect individuals, forming a deadly syndemic that disproportionately affects vulnerable populations. People living with HIV are up to 18 times more likely to develop active TB due to weakened immune defenses [4,5]. In 2023, TB was responsible for one-third of all AIDS-related deaths, highlighting the intertwined nature of these diseases [2]. Tackling HIV/TB co-infection requires integrated strategies that address both conditions simultaneously. Timely diagnosis and treatment of TB in HIV-positive individuals are critical but often hindered by overlapping symptoms and diagnostic challenges. Preventive interventions, such as isoniazid preventive therapy (IPT) and early initiation of ART, have demonstrated efficacy in reducing mortality [3]. Scaling these interventions, particularly in high-burden regions like sub-Saharan Africa and Southeast Asia, is crucial to controlling the dual epidemic [5]. Addressing HIV/TB coinfection also demands broader systemic changes, including reducing poverty, improving nutrition, and ensuring equitable access to healthcare. Community-based models of care that integrate TB and HIV services have shown success in improving outcomes and reducing stigma. Enhanced global collaboration, funding, and innovative approaches are needed to effectively address this dual burden and improve the lives of millions [2, 5].

The Atangana-Baleanu-Caputo (ABC) fractional derivative is revolutionizing how infectious diseases, such as tuberculosis, are modeled. Unlike standard calculus, it incorporates both historical and current data through a non-local, non-singular kernel. This unique approach makes it especially useful for capturing the slow progression, long periods of latency, and relapse tendencies characteristic of HIV and TB, which traditional models often struggle to represent effectively [12, 23]. By considering the influence of past conditions on present dynamics, the ABC derivative provides a more refined and accurate understanding of how infectious disease evolves over time. A key advantage of the ABC derivative is its stability, even in the context of complex systems. Traditional derivatives often fail to capture the

irregularities and multiple interacting factors present in diseases like HIV and TB, which unfold over different time scales. The ABC approach smooths these irregularities, allowing for more precise simulations of TB dynamics, such as treatment delays, partial adherence, and slow immune responses [8, 12]. This makes the ABC derivative a powerful tool for modeling real-world scenarios with greater accuracy, improving the representation of challenges faced in HIV-TB control and treatment.The non-local property of the ABC derivative also enables a better evaluation of the long-term effects of public health interventions. TB control and treatment often require sustained efforts over many years, so it is essential to understand how past interventions, such as vaccination programs or gaps in treatment, impact both current and future outcomes. By incorporating memory effects, the ABC derivative helps policymakers design strategies that consider the long-term implications of their decisions. Furthermore, it enhances the ability to assess public health interventions, such as how delays in vaccine distribution or uneven access to treatment can affect TB's spread and control over time. Ultimately, the ABC derivative bridges theoretical modeling with practical applications, offering a valuable tool for resource optimization and public health planning [12]. It provides a foundation for addressing HIV-TB with strategies that are both scientifically informed and grounded in real-world constraints. Bolaji et al. [6] developed a model and performed its qualitative analysis. They found that TB reinfection susceptibility could lead to backward bifurcation, complicating efforts to stabilize the disease-free state. Reducing reinfection susceptibility allowed for local stability of the disease-free equilibrium when the reproduction number was less than one. Sensitivity analysis identified key drivers of TB dynamics, including transmission rates, infectiousness modifiers, and treatment rates for latently infected individuals. Simulations indicated that prioritizing treatment for latently infected individuals, both singly and co-infected with HIV, effectively reduced the disease burden and HIV incidence, highlighting the importance of targeted interventions. A study by [9] applied fractional calculus to model the co-dynamics of COVID-19 and hepatitis B, using fractional-order derivatives. This model incorporated vaccination strategies and assessed their effects on disease transmission. By employing the Caputo derivative, the study analyzed the global stability of equilibrium points and performed sensitivity analyses. The results indicated that fractional models were more effective than traditional models in capturing the complex transmission dynamics of overlapping epidemics. The authors concluded that fractional-order derivatives offer a more adaptable and precise approach for understanding disease interactions and developing control strategies. In another study [10], a fractional piecewise derivative model was introduced to explore the dynamics of Rubella. The researchers integrated the Caputo and Atangana-Baleanu derivatives to address challenges such as memory effects and initial conditions. Validated with outbreak data, the model demonstrated greater accuracy in modeling disease spread compared to integer-order models. The study concluded that fractional calculus is a powerful tool for accurately replicating real-world epidemiological patterns, particularly in diseases with irregular transmission and long-lasting immunity effects.

A third study [11] focused on tuberculosis, employing the Caputo fractional derivative to assess the impact of treatment and control measures. The researchers utilized the homotopy perturbation method for numerical solutions and emphasized the role of memory effects in TB latency and relapse dynamics. The findings revealed that fractional models offer deeper insights into long-term TB transmission trends, improving the evaluation of treatment policies. The study concluded that using fractional derivatives in TB models enhances predictive capabilities and allows for better resource allocation in controlling the disease. Lastly, a study [13] applied a fractional-order model to analyze infection dynamics under network weighting and latency conditions. They proposed event-triggered impulsive control strategies based on infection rate thresholds and used the Atangana-Baleanu-Caputo derivative. Their results confirmed that these models maintained stability while avoiding issues like Zeno behavior. The conclusion highlighted the practicality of fractional models in creating precise, dynamic disease control strategies tailored to specific outbreak conditions. The study also explored the use of Mittag-Leffler functions to analyze the Atangana-Baleanu-Caputo fractional derivative, which incorporates non-local fading memory into dynamic systems. This memory effect allows for more accurate modeling of diseases like tuberculosis, where past conditions strongly influence the disease's current progression, particularly in its slow development, long latency, and relapse potential. This approach, through fractional calculus, offers a more comprehensive understanding of these processes than traditional models. Other relevant studies also support these findings [14–23].

The remaining part of the manuscript is structured as follows: Section 2 presents the preliminaries of

the fractional-order derivative used in the analysis of the model; Section 3 describes the HIV-TB model formulation; Section 4 discusses the existence and uniqueness of model solutions as well as its analysis; Section 5 analyzes the tuberculosis-only sub-model in terms of its basic reproduction number; Section 6 presents the numerical simulations of the model; and Section 7 provides the concluding remarks of the work.

2. Preliminary

Definition 2.1. ([23]) On the interval $\chi \in [0,1]$, by taking the function $f \in H^1(a,b),\ b > a$, so that ABC derivative is given by ${}_a^{ABC}D_\xi^\chi f(\xi) = \frac{\mathcal{A}(\chi)}{1-\chi}\int_a^\xi f'(\theta)E_\chi\left[-\chi\frac{(\xi-\theta)^\chi}{1-\chi}\right]d\theta$, With $\mathcal{A}(0) = \mathcal{A}(1) = 1$, where $\mathcal{A}(\chi)$ is a normalization function.

Definition 2.2. ([23]) On the interval $\chi \in [0,1]$, by taking the function $f \in H^1(a,b),\ b > a$, which is not differentiable, hence the Atangana-Baleanu fractional derivative in Riemann-Liouville sense is defined as ${}_a^{ABR}D_\xi^\chi f(\xi) = \frac{\mathcal{A}(\chi)}{1-\chi}\frac{d}{d\xi}\int_a^\xi f(\theta)E_\chi\left[-\chi\frac{(\xi-\theta)^\chi}{1-\chi}\right]d\theta$.

Definition 2.2. The ABC fractional derivative for the fractional integral of order χ is given by ${}_a^{AB}I_\xi^\chi f(\xi) = \frac{1-\chi}{\mathcal{A}(\chi)}f(\xi) + \frac{\chi}{\mathcal{A}(\chi)\Gamma(\chi)}\int_a^\xi f(y)(\xi-y)^{\chi-1}dy$.
If $\chi = 0$ and $\chi = 1$, the initial function and ordinary integral are obtained, below. In the next sections, we will investigate the Laplace transform operators and applied fundamental theorems associated with these derivatives. The connection between these operators and the Laplace Transform will be established. $L\left\{{}_0^{ABR}D_\xi^\chi\left[f(\xi)\right]\right\}(l) = \frac{\mathcal{A}(\chi)}{1-\chi}\frac{l^\chi L\{f(\xi)\}(l)}{l^\chi+\frac{\chi}{1-\chi}}$ and $L\left\{{}_0^{ABC}D_\xi^\chi\left[f(\xi)\right]\right\}(l) = \frac{\mathcal{A}(\chi)}{1-\chi}\frac{l^\chi L\{f(\xi)\}(l)-l^{\chi-1}f(0)}{l^\chi+\frac{\chi}{1-\chi}}$.

Theorem 2.1. ([12]) Consider the close interval [a, b] and use g to represent a continuous function defined on it. we establish the following inequality, which is true for any point lies in [a, b]:
$\left\|{}_0^{ABR}D_\xi^\chi\left[f(\xi)\right]\right\| < \frac{\mathcal{A}(\chi)}{1-\chi}\left\|f(\theta)\right\|$, where $\left\|f(\theta)\right\| = \max_{a\ \le\ \xi\le\ b}\left|f(\theta)\right|$.

Theorem 2.2. ([23]) The Riemann-Liouville and Caputo types of Atangana-Baleanu derivative exhibit the Lipchitz condition, which is best defined as given below $\left\|{}_0^{ABR}D_\xi^K\left[f(\xi)\right] - {}_0^{ABR}D_\xi^K\left[g(\xi)\right]\right\| \le H\left\|f(\xi)-g(\xi)\right\|$. And $\left\|{}_0^{ABC}D_\xi^\chi\left[f(\xi)\right] - {}_0^{ABC}D_\xi^\chi\left[g(\xi)\right]\right\| = H\left\|f(\xi)-g(\xi)\right\|$.

3. Mathematical Model

The total population denoted by $N(t)$ at any time t which is divided into thirteen compartments as stated in Table 1, so as to obtain:

$$N(t) = S(t) + E(t) + E_L(t) + E_{UL}(t) + I_{UA}(t) + T(t) + R(t) + I_H(t) + E_{TH}(t) + I_{HU}(t) + I_{HUA}(t) + I_{HDA}(t) + T_{HT}(t).$$

In co-infection models, it is often assumed that individuals infected with both tuberculosis (TB) and HIV can only transmit one disease at a time. This means they transmit either TB or HIV, but not both simultaneously [6]. This simplification helps streamline the model by focusing on the transmission of each disease separately, avoiding the complexities of dual transmission.

3.1. Transmissions by Singly Infected Individuals

Following effective contact with those infected with HIV only, individuals acquire HIV infection ($I_H(t)$ class), at the rate given by:

$$\dot{\lambda}_H = \beta_H\frac{I_H}{N}. \tag{3.1}$$

Where the transmission rate for HIV is β_H [6, 13].

Again, the acquisition of TB infection by humans from those in the I_{UA} and T compartments, at the rate λ_T is given by:

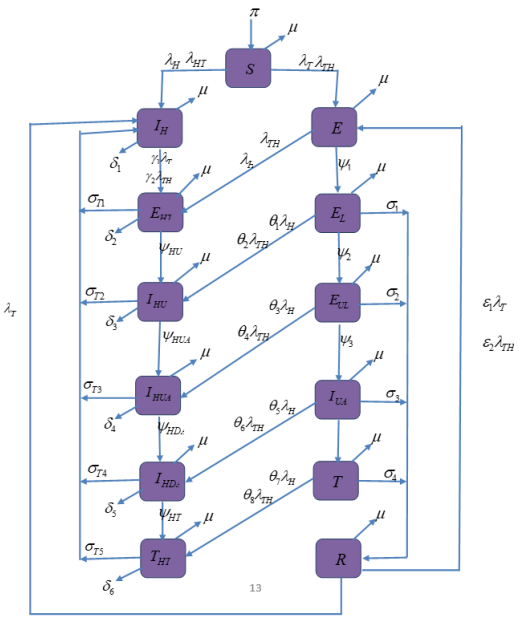

Figure 1: Schematic diagram of the model

$$\lambda_T = \beta_T \frac{(I_{UA} + \eta_1 T)}{N}. \tag{3.2}$$

Also , the transmission rate for TB is β_T and the η_1 for $\eta_1 \geq 1$ accounts for the relative infectiousness of those with secondary TB in comparison with those with primary TB, since it is assumed that infected humans in the secondary stage are more infectious than those in the primary stage of TB infection [6,14].

3.2. Transmission by Dual-Infected Individuals

TB is transmitted by dually infected humans at the rate given by:

$$\lambda_{TH} = \frac{\beta_T(\eta_2 I_{HUA} + \eta_3 I_{HDA})}{N}. \tag{3.3}$$

The increased infectiousness of individuals co-infected with HIV and tuberculosis in the primary stage of TB infection, compared to those with only primary TB, is represented by certain parameters η_2 and η_3. Similarly, the model accounts for the heightened infectiousness of individuals with both HIV and secondary TB, as opposed to those with secondary TB alone. This distinction arises from the relatively higher infectiousness of individuals with secondary TB compared to those with primary TB [6,13]. Due to relative infectiousness of those with secondary TB infection as compared to those with primary TB infections, it is pertinent to assume that $\eta_3 \geq \eta_2 > 1$. HIV transmission by dually infected individuals can occur at the rate given by:

$$\lambda_{HT} = \frac{\beta_H(E_{HT} + \varphi_1 I_{HU} + \varphi_2 I_{HUA} + \varphi_3 I_{HDA} + \varphi_4 I_{HT})}{N}. \tag{3.4}$$

Where the relative infectiousness of HIV-infected individuals with primary, secondary, early latent and late latent TB, respectively, compared to HIV-only infected individuals is accounted for by parameters φ_1,φ_2,φ_3 and φ_4 [6].

3.3. Description of How Model Equations were Formed

Based on the schematic diagram below, we formulate the following differential equations [6]:

Table 1: Description of state variables and parameters

State Variables	**Description**
S	Group of susceptible individuals
E	Group of infected individuals exposed to TB
E_L	Group of diagnosed latently infected individuals with TB
E_{UL}	Group of undiagnosed latently infected individuals with TB
I_{UA}	Group of undiagnosed actively infected individuals with TB
T	Group of diagnosed actively infected individuals with TB on prompt treatment
R	Group of recovered individuals
I_H	Group of infected individuals with HIV
E_{HT}	Group of dually infected individuals with diagnosed latent HIV and TB
I_{HU}	Group of dually infected individuals with HIV and undiagnosed latently infected TB
I_{HUA}	Group of dually infected individuals with HIV and undiagnosed active TB
I_{HDA}	Group of dually infected individuals with HIV diagnosed active TB
T_{HT}	Group of dually infected individuals with HIV and TB on prompt treatment for both disease
Parameter	**Description**
π	Recruitment rate into the susceptible class
μ	Natural death
$\beta_T(\beta_H)$	Contact rates for tuberculosis (HIV)
$\sigma_1, \sigma_2, \sigma_3, \sigma_4$	Treatment rates for singly infected individuals with latently-infected TB, undiagnosed latently-infected TB, undiagnosed actively-infected and diagnosed actively-infected individuals with TB on prompt treatment
$\sigma_{T1}, \sigma_{T2}, \sigma_{T3}, \sigma_{T4}$	Treatment rates for dually infected individuals with HIV and latently-infected TB, HIV and undiagnosed latently-infected with TB, HIV and undiagnosed actively-infected with TB, HIV and diagnosed actively-infected individuals with TB
$\psi_1, \psi_2, \psi_3, \psi_4$	Progression rates for singly infected individuals from exposed, diagnosed latently-infected, undiagnosed latently-infected, undiagnosed actively infected, diagnosed actively infected with TB on prompt treatment to classes E_L, E_{UL}, I_{UA}, T and R respectively
$\psi_{HU}, \psi_{HUA}, \psi_{HDA}, \psi_{HT}$	Progression rates for dually infected individuals from classes E_{HT}, I_{HU}, I_{HUA}, I_{HDA}, and T_{HT} to classes I_{HU}, I_{HUA}, I_{HDA}, T_{HT} respectively
σ_1, σ_2	Modification parameters that account for variability in susceptibility of recovered individuals to TB infection
γ_1, γ_2	Modification parameters that accounts for the susceptibility of recovered individuals to TB infection
$\theta_1, \theta_2, \theta_3, \theta_4, \theta_5, \theta_6, \theta_7, \theta_8$	Modification parameters that account for the susceptibility of TB-infected individuals to HIV infection
η_1, η_2, η_3	Modification parameters that account for the infectiousness of infected individuals with TB only, HIV and undiagnosed actively infected TB, HIV and diagnosed actively-infected TB respectively
$\varphi_1, \varphi_2, \varphi_3, \varphi_4$	Modification parameters that account for the infectiousness of dually infected individuals
$\delta_1, \delta_2, \delta_3, \delta_4, \delta_5, \delta_6$	Disease-induced death rates due to HIV with TB co-infection
γ	Efficacy of quarantine, hospitalization/isolation and care in intensive care unit (ICU) form transmitting infections ($0 \leq \gamma \leq 1$)
$\eta_S(\eta_H)$	Modification parameters for the assumed reduction in infectiousness of individuals who are asymptomatic in hospital/isolation centre

$$
\begin{aligned}
\dot{S} &= \pi - \lambda_T S - \lambda_\mu S - \lambda_{TH} S - \lambda_{HT} S - \mu S,\\
\dot{E} &= \lambda_T S + \lambda_{TH} S + \sigma_1 \lambda_T R + \sigma_2 \lambda_{TH} R - (\psi_1 + \mu) E - \lambda_H E - \lambda_{HT} E,\\
\dot{E}_L &= \psi_1 E - (\psi_2 + \sigma_1 + \mu) E_L - \theta_1 \lambda_H E_L - \theta_2 \lambda_{HT} E_L,\\
\dot{E}_{UL} &= \psi_2 E_L - (\psi_3 + \sigma_2 + \mu) E_{UL} - \theta_3 \lambda_H E_{UL} - \theta_4 \lambda_H E_{UL},\\
\dot{I}_{UA} &= \psi_3 E_{UL} - (\psi_4 + \sigma_3 + \mu) I_{UA} - \theta_5 \lambda_H I_{UA} - \theta_6 \lambda_{HT} I_{UA},\\
\dot{T} &= \psi_4 I_{UA} - (\psi_5 + \sigma_4 + \mu) T - \theta_7 \lambda_H T - \theta_8 \lambda_{HT} T,\\
\dot{R} &= \sigma_1 E_L + \sigma_2 E_{UL} + \sigma_3 I_{UA} + \sigma_4 T - \sigma_1 \lambda_T R - \mu R - \lambda_H R - \sigma_2 \lambda_{TH} R - \lambda_{HT} R,\\
\dot{I}_H &= \lambda_H S + \lambda_{HT} S + \lambda_H R + \lambda_{HT} R - \sigma_1 \lambda_T I_H - \sigma_2 \lambda_{TH} I_H - (\mu + \sigma_1) I_H +\\
&\quad \sigma_{T1} E_{HT} + \sigma_{T2} I_{HU} + \sigma_{T3} I_{HUA} + \sigma_{T4} I_{HDA} + \sigma_{T5} T_{HT},\\
\dot{E}_{HT} &= \sigma_1 \lambda_T I_H + \sigma_2 \lambda_{TH} I_H + \lambda_{HT} E - (\psi_{HU} + \sigma_{T1} + \sigma_2 + \mu) E_{HT},\\
\dot{I}_{HU} &= \psi_{HU} E_{HT} + \theta_1 \lambda_H E_L + \theta_2 \lambda_{HT} E_L - (\psi_{HUA} + \sigma_3 + \sigma_{T2} + \mu) I_{HU},\\
\dot{I}_{HUA} &= \psi_{HUA} I_{HU} + \theta_3 \lambda_H E_{UL} + \theta_4 \lambda_{HT} E_{UL} - (\psi_{HDA} + \sigma_{T3} + \sigma_4 + \mu) I_{HUA},\\
\dot{I}_{HDA} &= \psi_{HDA} I_{HUA} + \theta_5 \lambda_H I_{UA} + \theta_6 \lambda_{HT} I_{UA} - (\psi_{HT} + \sigma_{T3} + \sigma_5 + \mu) I_{HDA},\\
\dot{T}_{HT} &= \psi_{HU} I_{HDA} + \theta_7 \lambda_H T + \theta_8 \lambda_{HT} T - (\sigma_{T5} + \sigma_6 + \mu) T_{HT}.
\end{aligned}
\tag{3.5}
$$

Given that derivatives of fractional order represent epidemiological patterns better than classical order cases. We therefore modify the HIV-TB model (3.5) in terms of the ABC derivative given as follows

$$
\begin{aligned}
{}_0^{ABC}D_\xi^\chi S(\xi) &= \pi - \lambda_T S - \lambda_\mu S - \lambda_{TH} S - \lambda_{HT} S - \mu S,\\
{}_0^{ABC}D_\xi^\chi E(\xi) &= \lambda_T S + \lambda_{TH} S + \sigma_1 \lambda_T R + \sigma_2 \lambda_{TH} R - (\psi_1 + \mu) E - \lambda_H E - \lambda_{HT} E,\\
{}_0^{ABC}D_\xi^\chi E_L(\xi) &= \psi_1 E - (\psi_2 + \sigma_1 + \mu) E_L - \theta_1 \lambda_H E_L - \theta_2 \lambda_{HT} E_L,\\
{}_0^{ABC}D_\xi^\chi E_{UL}(\xi) &= \psi_2 E_L - (\psi_3 + \sigma_2 + \mu) E_{UL} - \theta_3 \lambda_H E_{UL} - \theta_4 \lambda_H E_{UL},\\
{}_0^{ABC}D_\xi^\chi I_{UA}(\xi) &= \psi_3 E_{UL} - (\psi_4 + \sigma_3 + \mu) I_{UA} - \theta_5 \lambda_H I_{UA} - \theta_6 \lambda_{HT} I_{UA},\\
{}_0^{ABC}D_\xi^\chi T(\xi) &= \psi_4 I_{UA} - (\psi_5 + \sigma_4 + \mu) T - \theta_7 \lambda_H T - \theta_8 \lambda_{HT} T,\\
{}_0^{ABC}D_\xi^\chi R(\xi) &= \sigma_1 E_L + \sigma_2 E_{UL} + \sigma_3 I_{UA} + \sigma_4 T - \sigma_1 \lambda_T R - \mu R - \lambda_H R - \sigma_2 \lambda_{TH} R,\\
{}_0^{ABC}D_\xi^\chi I_H(\xi) &= \lambda_H S + \lambda_{HT} S + \lambda_H R + \lambda_{HT} R - \sigma_1 \lambda_T I_H - \sigma_2 \lambda_{TH} I_H - (\mu + \sigma_1) I_H\\
&\quad + \sigma_{T1} E_{HT} + \sigma_{T2} I_{HU} + \sigma_{T3} I_{HUA} + \sigma_{T4} I_{HDA} + \sigma_{T5} T_{HT},\\
{}_0^{ABC}D_\xi^\chi E_{HT}(\xi) &= \sigma_1 \lambda_T I_H + \sigma_2 \lambda_{TH} I_H + \lambda_{HT} E - (\psi_{HU} + \sigma_{T1} + \sigma_2 + \mu) E_{HT},\\
{}_0^{ABC}D_\xi^\chi I_{HU}(\xi) &= \psi_{HU} E_{HT} + \theta_1 \lambda_H E_L + \theta_2 \lambda_{HT} E_L - (\psi_{HUA} + \sigma_3 + \sigma_{T2} + \mu) I_{HU},\\
{}_0^{ABC}D_\xi^\chi I_{HUA}(\xi) &= \psi_{HUA} I_{HU} + \theta_3 \lambda_H E_{UL} + \theta_4 \lambda_{HT} E_{UL} - (\psi_{HDA} + \sigma_{T3} + \sigma_4 + \mu) I_{HUA},\\
{}_0^{ABC}D_\xi^\chi I_{HDA}(\xi) &= \psi_{HDA} I_{HUA} + \theta_5 \lambda_H I_{UA} + \theta_6 \lambda_{HT} I_{UA} - (\psi_{HT} + \sigma_{T3} + \sigma_5 + \mu) I_{HDA},\\
{}_0^{ABC}D_\xi^\chi T_{HT}(\xi) &= \psi_{HU} I_{HDA} + \theta_7 \lambda_H T + \theta_8 \lambda_{HT} T - (\sigma_{T5} + \sigma_6 + \mu) T_{HT}.
\end{aligned}
\tag{3.6}
$$

Subject to initial conditions

$$S(0) = S_0,\ E(0) = E_0,\ E_L(0) = E_{L0},\ E_{UL}(0) = E_{UL0},\ I_{UA}(0) = I_{UA0},$$

$$T(0) = T_0,\ R(0) = R_0,\ I_H(0) = I_{H0},\ E_{HT}(0) = E_{HT0},\ I_{HU}(0) = I_{HU0},\ I_{HUA(0)} = I_{HUA0},$$

$$I_{HDA}(0) = I_{HDA0},\ T_{HT}(0) = T_{HT0}.$$

3.4. Model Assumptions

1. Individuals infected with tuberculosis can recover through effective treatment. However, we assume that recovery from HIV through treatment is not possible, reflecting the current limitations of medical interventions for HIV [33, 35].

2. Natural death occurs uniformly across all population compartments at a constant rate. This ensures consistency in modeling population dynamics regardless of health status or infection type [35].

3. The death rate attributable to disease progression is uniform across all infected compartments, regardless of whether individuals are infected with TB, HIV, or both.

4. To focus on the early and intermediate stages of HIV infection, we excluded individuals who progress from HIV to AIDS after a period. This simplification isolates the dynamics of co-infection without complicating the model with late-stage disease progression [36].

5. Based on findings that approximately 80% of individuals infected with HIV are highly susceptible to TB infection [35], we assume that individuals with HIV have an increased risk of acquiring TB. This reflects the strong epidemiological association in which HIV-induced immunosuppression facilitates the progression from latent to active TB.

4. Existence and Uniqueness of Analysis

Solving nonlinear equations presents a significant challenge in the field of differential calculus, particularly when dealing with complex systems. The fractional-order model being studied exhibits considerable nonlinearity, making it difficult to obtain exact solutions [23]. Consequently, our primary objective is to address the existence and uniqueness of solutions for this model. To tackle this, we apply the fixed point theorem, a robust technique commonly used to demonstrate the existence of solutions in nonlinear equations across various mathematical frameworks [10, 12]. This approach helps us explore the system's behavior and gain a deeper understanding of its properties, particularly in the context of its dynamics. On the interval q, suppose that $p = K(q) \times K(q)$, where the Banach space $K(q)$ of continuous real value functions is defined with the norm

$$\begin{aligned}\|S,\ E,\ E_L,\ E_{UL},\ I_{UA},\ T,\ R,\ I_H,\ E_{HT},\ I_{HU},\ I_{HUA},\ I_{HDA},\ T_{HT}\| &= \|S\| + \|E\| + \|E_{UL}\| \\ &+ \|I_{UA}\| + \|T\| + \|R\| + \|I_H\| + \|E_{HT}\| + \|I_{HU}\| + \|I_{UA}\| + \|I_{HUA}\| + \|I_{HDA}\| + \|T_{HT}\|.\end{aligned}$$

Where,

$$\|S\| = \sup\{|S(\xi)| : \xi \in q\},$$

$$\|E\| = \sup\{|E(\xi)| : \xi \in q\},$$

$$\|E_{UL}\| = \sup\{|E_{UL}(\xi)| : \xi \in q\},$$

$$\|I_{UA}\| = \sup\{|I_{UA}(\xi)| : \xi \in q\},$$

$$\|T\| = \sup\{|T(\xi)| : \xi \in q\},$$

$$\|R\| = \sup\{|R(\xi)| : \xi \in q\},$$

$$\|I_H\| = \sup\{|I_H(\xi)| : \xi \in q\},$$

$$\|E_{HT}\| = \sup\{|E_{HT}(\xi)| : \xi \in q\},$$

$$\|I_{HU}\| = \sup\{|I_{HU}(\xi)| : \xi \in q\},$$

$$\|I_{HUA}\| = \sup\{|I_{HUA}(\xi)| : \xi \in q\},$$

$$\|I_{HDA}\| = \sup\{|I_{HDA}(\xi)| : \xi \in q\},$$

$$\|T_{HT}\| = \sup\{|T_{HT}(\xi)| : \xi \in q\}.$$

The model (3.6) is transformed into the following equation by taking the Atangana-Baleanu fractional integral into account.

$$E(\xi)-E(0)=\frac{1-\chi}{\mathcal{A}(\chi)}\left\{\lambda_T S+\lambda_{TH}S+\sigma_1\lambda_T R+\sigma_2\lambda_{TH}R-(\psi_1+\mu)E-\lambda_H E-\lambda_{HT}E\right\}$$
$$+\frac{\chi}{\mathcal{A}(\chi)\Gamma(\chi)}\int_0^{\xi}(\xi-y)^{\chi-1}\left\{\lambda_T S+\lambda_{TH}S+\sigma_1\lambda_T R+\sigma_2\lambda_{TH}R-(\psi_1+\mu)E-\lambda_H E-\lambda_{HT}E\right\}dy,$$

$$\begin{aligned}
E_L(\xi)-E_L(0)&=\frac{1-\chi}{\mathcal{A}(\chi)}\left\{\psi_1 E-(\psi_2+\sigma_1+\mu)E_L-\theta_1\lambda_H E_L-\theta_2\lambda_{HT}E_L\right\}\\
&\quad+\frac{\chi}{\mathcal{A}(\chi)\Gamma(\chi)}\int_0^{\xi}(\xi-y)^{\chi-1}\left\{\psi_1 E-(\psi_2+\sigma_1+\mu)E_L-\theta_1\lambda_H E_L-\theta_2\lambda_{HT}E_L\right\}dy,
\end{aligned}\tag{4.1}$$

$$E_{UL}(\xi)-E_{UL}(0)=\frac{1-\chi}{\mathcal{A}(\chi)}\left\{\psi_2 E_L-(\psi_3+\sigma_2+\mu)E_{UL}-\theta_3\lambda_H E_{UL}-\theta_4\lambda_H E_{UL}\right\}$$
$$+\frac{\chi}{\mathcal{A}(\chi)\Gamma(\chi)}\int_0^{\xi}(\xi-y)^{\chi-1}\left\{\psi_2 E_L-(\psi_3+\sigma_2+\mu)E_{UL}-\theta_3\lambda_H E_{UL}-\theta_4\lambda_H E_{UL}\right\}dy,$$
$$I_{UA}(\xi)-I_{UA}(0)=\frac{1-\chi}{\mathcal{A}(\chi)}\left\{\psi_3 E_{UL}-(\psi_4+\sigma_3+\mu)I_{UA}-\theta_5\lambda_H I_{UA}-\theta_6\lambda_{HT}I_{UA}\right\}$$
$$+\frac{\chi}{\mathcal{A}(\chi)\Gamma(\chi)}\int_0^{\xi}(\xi-y)^{\chi-1}\left\{\psi_3 E_{UL}-(\psi_4+\sigma_3+\mu)I_{UA}-\theta_5\lambda_H I_{UA}-\theta_6\lambda_{HT}I_{UA}\right\}dy,$$
$$T(\xi)-T(0)=\frac{1-\chi}{\mathcal{A}(\chi)}\left\{\psi_4 I_{UA}-(\psi_5+\sigma_4+\mu)T-\theta_7\lambda_H T-\theta_8\lambda_{HT}T\right\}$$
$$+\frac{\chi}{\mathcal{A}(\chi)\Gamma(\chi)}\int_0^{\xi}(\xi-y)^{\chi-1}\left\{\psi_4 I_{UA}-(\psi_5+\sigma_4+\mu)T-\theta_7\lambda_H T-\theta_8\lambda_{HT}T\right\}dy,$$
$$R(\xi)-R(0)=\frac{1-\chi}{\mathcal{A}(\chi)}\left\{\sigma_1 E_L+\sigma_2 E_{UL}+\sigma_3 I_{UA}+\sigma_4 T-\sigma_1\lambda_T R-\mu R-\lambda_H R-\sigma_2\lambda_{TH}R\right\}$$
$$+\frac{\chi}{\mathcal{A}(\chi)\Gamma(\chi)}\int_0^{\xi}(\xi-y)^{\chi-1}\left\{\sigma_1 E_L+\sigma_2 E_{UL}+\sigma_3 I_{UA}+\sigma_4 T-\sigma_1\lambda_T R-\mu R-\lambda_H R-\sigma_2\lambda_{TH}R\right\}dy,$$
$$I_H(\xi)-I_H(0)=\frac{1-\chi}{\mathcal{A}(\chi)}\left\{\begin{matrix}\lambda_H S+\lambda_{HT}S+\lambda_H R+\lambda_{HT}R-\sigma_1\lambda_T I_H-\sigma_2\lambda_{TH}I_H-(\mu+\sigma_1)I_H+\\,\sigma_{T1}E_{HT}+\sigma_{T2}I_{HU}+\sigma_{T3}I_{HUA}+\sigma_{T4}I_{HDA}+\sigma_{T5}T_{HT}\end{matrix}\right\}$$
$$+\frac{\chi}{\mathcal{A}(\chi)\Gamma(\chi)}\int_0^{\xi}(\xi-y)^{\chi-1}\left\{\begin{matrix}\lambda_H S+\lambda_{HT}S+\lambda_H R+\lambda_{HT}R-\sigma_1\lambda_T I_H-\sigma_2\lambda_{TH}I_H-(\mu+\sigma_1)I_H+\\,\sigma_{T1}E_{HT}+\sigma_{T2}I_{HU}+\sigma_{T3}I_{HUA}+\sigma_{T4}I_{HDA}+\sigma_{T5}T_{HT}\end{matrix}\right\}dy,$$
$$E_{HT}(\xi)-E_{HT}(0)=\frac{1-\chi}{\mathcal{A}(\chi)}\left\{\sigma_1\lambda_T I_H+\sigma_2\lambda_{TH}I_H+\lambda_{HT}E-(\psi_{HU}+\sigma_{T1}+\sigma_2+\mu)E_{HT}\right\}$$
$$+\frac{\chi}{\mathcal{A}(\chi)\Gamma(\chi)}\int_0^{\xi}(\xi-y)^{\chi-1}\left\{\sigma_1\lambda_T I_H+\sigma_2\lambda_{TH}I_H+\lambda_{HT}E-(\psi_{HU}+\sigma_{T1}+\sigma_2+\mu)E_{HT}\right\}dy,$$
$$I_{HU}(\xi)-I_{HU}(0)=\frac{1-\chi}{\mathcal{A}(\chi)}\left\{\psi_{HU}E_{HT}+\theta_1\lambda_H E_L+\theta_2\lambda_{HT}E_L-(\psi_{HUA}+\sigma_3+\sigma_{T2}+\mu)I_{HU}\right\}$$
$$+\frac{\chi}{\mathcal{A}(\chi)\Gamma(\chi)}\int_0^{\xi}(\xi-y)^{\chi-1}\left\{\psi_{HU}E_{HT}+\theta_1\lambda_H E_L+\theta_2\lambda_{HT}E_L-(\psi_{HUA}+\sigma_3+\sigma_{T2}+\mu)I_{HU}\right\}dy,$$
$$H_{HUA}(\xi)-H_{HUA}(0)=\frac{1-\chi}{\mathcal{A}(\chi)}\left\{\psi_{HUA}I_{HU}+\theta_3\lambda_H E_{UL}+\theta_4\lambda_{HT}E_{UL}-(\psi_{HDA}+\sigma_{T3}+\sigma_4+\mu)I_{HUA}\right\}$$
$$+\frac{\chi}{\mathcal{A}(\chi)\Gamma(\chi)}\int_0^{\xi}(\xi-y)^{\chi-1}\left\{\psi_{HUA}I_{HU}+\theta_3\lambda_H E_{UL}+\theta_4\lambda_{HT}E_{UL}-(\psi_{HDA}+\sigma_{T3}+\sigma_4+\mu)I_{HUA}\right\}dy,$$
$$I_{HDA}(\xi)-I_{HDA}(0)=\frac{1-\chi}{\mathcal{A}(\chi)}\left\{\psi_{HDA}I_{HUA}+\theta_5\lambda_H I_{UA}+\theta_6\lambda_{HT}I_{UA}-(\psi_{HT}+\sigma_{T3}+\sigma_5+\mu)I_{HDA}\right\}$$
$$+\frac{\chi}{\mathcal{A}(\chi)\Gamma(\chi)}\int_0^{\xi}(\xi-y)^{\chi-1}\left\{\psi_{HDA}I_{HUA}+\theta_5\lambda_H I_{UA}+\theta_6\lambda_{HT}I_{UA}-(\psi_{HT}+\sigma_{T3}+\sigma_5+\mu)I_{HDA}\right\}dy,$$

$$T_{HT}(\xi) - T_{HT}(0) = \frac{1-\chi}{\mathcal{A}(\chi)}\{\psi_{HU}I_{HDA} + \theta_7\lambda_H T + \theta_8\lambda_{HT}T - (\sigma_{T5}+\sigma_6+\mu)T_{HT}\}$$
$$+ \frac{\chi}{\mathcal{A}(\chi)\Gamma(\chi)}\int_0^{\xi}(\xi-y)^{\chi-1}\{\psi_{HU}I_{HDA} + \theta_7\lambda_H T + \theta_8\lambda_{HT}T - (\sigma_{T5}+\sigma_6+\mu)T_{HT}\}\,dy.$$

Simplifying (4.1), we have

$$K_1(\xi,\ S) = \pi - \lambda_T S - \lambda_\mu S - \lambda_{TH}S - \lambda_{HT}S - \mu S,$$

$$K_2(\xi,\ E) = \lambda_T S + \lambda_{TH}S + \sigma_1\lambda_T R + \sigma_2\lambda_{TH}R - (\psi_1+\mu)E - \lambda_H E - \lambda_{HT}E,$$

$$K_3(\xi,\ E_L) = \psi_1 E - (\psi_2+\sigma_1+\mu)E_L - \theta_1\lambda_H E_L - \theta_2\lambda_{HT}E_L,$$

$$K_4(\xi,\ E_{UL}) = \psi_2 E_L - (\psi_3+\sigma_2+\mu)E_{UL} - \theta_3\lambda_H E_{UL} - \theta_4\lambda_H E_{UL},$$

$$K_5(\xi,\ I_{UA}) = \psi_3 E_{UL} - (\psi_4+\sigma_3+\mu)I_{UA} - \theta_5\lambda_H I_{UA} - \theta_6\lambda_{HT}I_{UA},$$

$$K_6(\xi,\ T) = \psi_4 I_{UA} - (\psi_5+\sigma_4+\mu)T - \theta_7\lambda_H T - \theta_8\lambda_{HT}T,$$

$$K_7(\xi,\ R) = \sigma_1 E_L + \sigma_2 E_{UL} + \sigma_3 I_{UA} + \sigma_4 T - \sigma_1\lambda_T R - \mu R - \lambda_H R - \sigma_2\lambda_{TH}R,$$

$$K_8(\xi,\ I_H) = \lambda_H S + \lambda_{HT}S + \lambda_H R + \lambda_{HT}R - \sigma_1\lambda_T I_H - \sigma_2\lambda_{TH}I_H - (\mu+\sigma_1)I_H$$
$$+ \sigma_{T1}E_{HT} + \sigma_{T2}I_{HU} + \sigma_{T3}I_{HUA} + \sigma_{T4}I_{HDA} + \sigma_{T5}T_{HT},$$

$$K_9(\xi,\ E_{HT}) = \sigma_1\lambda_T I_H + \sigma_2\lambda_{TH}I_H + \lambda_{HT}E - (\psi_{HU}+\sigma_{T1}+\sigma_2+\mu)E_{HT},$$

$$K_{10}(\xi,\ I_{HU}) = \psi_{HU}E_{HT} + \theta_1\lambda_H E_L + \theta_2\lambda_{HT}E_L - (\psi_{HUA}+\sigma_3+\sigma_{T2}+\mu)I_{HU},$$

$$K_{11}(\xi,\ I_{HUA}) = \psi_{HUA}I_{HU} + \theta_3\lambda_H E_{UL} + \theta_4\lambda_{HT}E_{UL} - (\psi_{HDA}+\sigma_{T3}+\sigma_4+\mu)I_{HUA},$$

$$K_{12}(\xi,\ I_{HDA}) = \psi_{HDA}I_{HUA} + \theta_5\lambda_H I_{UA} + \theta_6\lambda_{HT}I_{UA} - (\psi_{HT}+\sigma_{T3}+\sigma_5+\mu)I_{HDA},$$

$$K_{13}(\xi,\ T_{HT}) = \psi_{HU}I_{HDA} + \theta_7\lambda_H T + \theta_8\lambda_{HT}T - (\sigma_{T5}+\sigma_6+\mu)T_{HT}.$$

Theorem 4.1. If the aforementioned inequality holds: $0 \le \beta_1 < 1$, $0 \le \beta_2 < 1$, $0 \le \beta_3 < 1$, $0 \le \beta_4 < 1$, $0 \le \beta_5 < 1$, $0 \le \beta_6 < 1$, $0 \le \beta_7 < 1$, $0 \le \beta_8 < 1$, $0 \le \beta_9 < 1$, $0 \le \beta_{10} < 1$, $0 \le \beta_{11} < 1$, $0 \le \beta_{12} < 1$, $0 \le \beta_{13} < 1$.

Then the kernels $k_1, k_2, k_3, k_4, k_5, k_6, k_7, k_8, k_9, k_{10}, k_{11}, k_{12}$, and k_{13} satisfy the Lipchitz condition and contradiction.

Proof. By taking the kernel $\kappa_1(\xi,\ S) = \pi - \lambda_T S - \lambda_\mu S - \lambda_{TH}S - \lambda_{HT}S - \mu S$.

Let S_H and S_{H1} be any two functions, so that:

$$\|\kappa_1(\xi,\ S(\xi)) - \kappa_1(\xi,\ S_1(\xi))\|$$
$$= \|\pi - \lambda_T S - \lambda_\mu S - \lambda_{TH}S - \lambda_{HT}S - \mu S - (\pi - \lambda_T S_1 - \lambda_\mu S_1 - \lambda_{TH}S_1 - \lambda_{HT}S_1 - \mu S_1)\|$$
$$\le \|-(\lambda_T + \lambda_\mu + \lambda_{TH} + \lambda_{HT} + \mu)\|\,\|S_H(\xi) - S_{H1}(\xi)\|$$
$$\le \left\|-\left(\frac{\beta_T I_{UA}}{N} + \frac{\beta_T\eta_1 T}{N} + \frac{\beta_T\eta_2 I_{HUA}}{N} + \frac{\beta_T\eta_3 I_{HDA}}{N} + \frac{\beta_H E_{HT}}{N} + \frac{\beta_H\phi_1 I_{HU}}{N} + \frac{\beta_H\phi_2 I_{HUA}}{N}\right.\right.$$
$$\left.\left. + \frac{\beta_H\phi_3 I_{HDA}}{N} + \frac{\beta_H\phi_4 T_{HT}}{N} + \lambda_u + \mu_H\right)\right\|\,\|S(\xi) - S_1(\xi)\|$$

$$\leq \left(\beta_T \left\|\frac{I_{UA}(\xi)}{N}\right\| + \beta_T\eta_1 \left\|\frac{T(\xi)}{N}\right\| + \beta_T\eta_2 \left\|\frac{I_{HUA}(\xi)}{N}\right\| + \beta_T\eta_3 \left\|\frac{I_{HDA}(\xi)}{N}\right\| + \beta_H \left\|\frac{E_{HT}(\xi)}{N}\right\|\right.$$
$$+ \beta_H\phi_1 \left\|\frac{I_{HU}(\xi)}{N}\right\| + \beta_H\phi_2 \left\|\frac{I_{HUA}(\xi)}{N}\right\|$$
$$\left.+\beta_H\phi_3 \left\|\frac{I_{HDA}(\xi)}{N}\right\| + \beta_H\phi_4 \left\|\frac{T_{HT}(\xi)}{N}\right\| + \lambda_u + \mu_H\right) \|S(\xi) - S_1(\xi)\|$$
$$\leq (\beta_T P_5 + \beta_T\eta_1 P_6 + \beta_T\eta_2 P_{11} + \beta_T\eta_3 P_{12} + \beta_H P_9 + \beta_H\phi_1 P_{10} + \beta_H\phi_2 P_{11} + \beta_H\phi_3 P_{12} + \beta_H\phi_4 P_{13}$$
$$+\lambda_u + \mu_H) \|S(\xi) - S_1(\xi)\|$$
$$\leq \beta_1 \|S(\xi) - S_1(\xi)\|,$$

$$\beta_1 = (\beta_T P_5 + \beta_T\eta_1 P_6 + \beta_T\eta_2 P_{11} + \beta_T\eta_3 P_{12} + \beta_H P_9 + \beta_H\phi_1 P_{10}$$
$$+\beta_H\phi_2 P_{11} + \beta_H\phi_3 P_{12} + \beta_H\phi_4 P_{13} + \lambda_u + \mu_H),$$

where $P_1 = \max_{\xi\in J} \|S(\xi)\|$, $P_2 = \max_{\xi\in J} \|E(\xi)\|$, $P_3 = \max_{\xi\in J} \|E_L(\xi)\|$, $P_4 = \max_{\xi\in J} \|E_{UL}(\xi)\|$, $P_5 = \max_{\xi\in J} \|I_{UA}(\xi)\|$, $P_6 = \max_{\xi\in J} \|T(\xi)\|$, $P_7 = \max_{\xi\in J} \|R(\xi)\|$, $P_8 = \max_{\xi\in J} \|I_H(\xi)\|$, $P_9 = \max_{\xi\in J} \|E_{HT}(\xi)\|$, $P_{10} = \max_{\xi\in J} \|I_{HU}(\xi)\|$, $P_{11} = \max_{\xi\in J} \|I_{HUA}(\xi)\|$, $P_{12} = \max_{\xi\in J} \|I_{HDA}(\xi)\|$, $P_{13} = \max_{\xi\in J} \|T_{HT}(\xi)\|$.

Are bounded functions, we have

$\|\kappa_1(\xi, S(\xi)) - \kappa_1(\xi, S_1(\xi))\| \leq \beta_1 \|S(\xi) - S_1(\xi)\|$.

Thus κ_1 satisfied the Lipchitz condition, and if $0 \leq \beta_1 < 1$, then it is also a contraction for κ_1. In the same manner, the Lipchitz condition is satisfied by other kernels:

$$\|\kappa_2(\xi, E(\xi)) - \kappa_2(\xi, E_1(\xi))\| \leq \beta_2 \|E(\xi) - E_1(\xi)\|,$$

$$\|\kappa_3(\xi, E_L(\xi)) - \kappa_3(\xi, E_{L1}(\xi))\| \leq \beta_3 \|E_L(\xi) - E_{L1}(\xi)\|,$$

$$\|\kappa_4(\xi, E_{UL}(\xi)) - \kappa_4(\xi, E_{UL}(\xi))\| \leq \beta_4 \|E_{UL}(\xi) - E_{UL1}(\xi)\|,$$

$$\|\kappa_5(\xi, I_{UA}(\xi)) - \kappa_5(\xi, I_{UA1}(\xi))\| \leq \beta_5 \|I_{UA}(\xi) - I_{UA1}(\xi)\|,$$

$$\|\kappa_6(\xi, T(\xi)) - \kappa_6(\xi, T_1(\xi))\| \leq \beta_6 \|T(\xi) - T_1(\xi)\|.$$

$$\|\kappa_7(\xi, R(\xi)) - \kappa_7(\xi, R_1(\xi))\| \leq \beta_7 \|R(\xi) - R_1(\xi)\|,$$

$$\|\kappa_8(\xi, I_H(\xi)) - \kappa_8(\xi, I_H(\xi))\| \leq \beta_8 \|I_H(\xi) - I_{H1}(\xi)\|,$$

$$\|\kappa_9(\xi, E_{HT}(\xi)) - \kappa_9(\xi, E_{H1}(\xi))\| \leq \beta_9 \|E_{HT}(\xi) - E_{HT1}(\xi)\|,$$

$$\|\kappa_{10}(\xi, I_{HU}(\xi)) - \kappa_{10}(\xi, I_{HU1}(\xi))\| \leq \beta_{10} \|I_{HU}(\xi) - I_{HU1}(\xi)\|,$$

$$\|\kappa_{11}(\xi, I_{HUA}(\xi)) - \kappa_{11}(\xi, I_{HUA1}(\xi))\| \leq \beta_{11} \|I_{HUA}(\xi) - I_{HUA1}(\xi)\|,$$

$$\|\kappa_{12}(\xi, I_{HDA}(\xi)) - \kappa_{12}(\xi, I_{HDA1}(\xi))\| \leq \beta_{12} \|I_{12}(\xi) - I_{12}(\xi)\|,$$

$$\|\kappa_{13}(\xi, T_{HT}(\xi)) - \kappa_{13}(\xi, T_{HT1}(\xi))\| \leq \beta_{13} \|T_{HT}(\xi) - T_{HT1}(\xi)\|.$$

By taking the kernel for the model into consideration, we write (4.1) as follows:

$$
\begin{aligned}
S(\xi) &= S(0) + \tfrac{1-\chi}{\mathcal{A}(\chi)}\kappa_1(\xi, S) + \tfrac{\chi}{\mathcal{A}(\chi)\Gamma(\chi)}\int_0^\xi (\xi-y)^{\chi-1}\kappa_1(y, S)\,dy,\\
E(\xi) &= E(0) + \tfrac{1-\chi}{\mathcal{A}(\chi)}\kappa_2(\xi, E) + \tfrac{\chi}{\mathcal{A}(\chi)\Gamma(\chi)}\int_0^\xi (\xi-y)^{\chi-1}\kappa_2(y, E)\,dy,\\
E_L(\xi) &= E_L(0) + \tfrac{1-\chi}{\mathcal{A}(\chi)}\kappa_3(\xi, E_L) + \tfrac{\chi}{\mathcal{A}(\chi)\Gamma(\chi)} + \int_0^\xi (\xi-y)^{\chi-1}\kappa_3(y, E_L)\,dy,\\
E_{UL}(\xi) &= E_{UL}(0) + \tfrac{1-\chi}{\mathcal{A}(\chi)}\kappa_4(\xi, E_{UL}) + \tfrac{\chi}{\mathcal{A}(\chi)\Gamma(\chi)}\int_0^\xi (\xi-y)^{\chi-1}\kappa_4(y, E_{UL})\,dy,\\
I_{UA}(\xi) &= I_{UA}(0) + \tfrac{1-\chi}{\mathcal{A}(\chi)}\kappa_5(\xi, I_{UA}) + \tfrac{\chi}{\mathcal{A}(\chi)\Gamma(\chi)}\int_0^\xi (\xi-y)^{\chi-1}\kappa_5(y, I_{UA})\,dy,\\
T(\xi) &= T(0) + \tfrac{1-\chi}{\mathcal{A}(\chi)}\kappa_6(\xi, T) + \tfrac{\chi}{\mathcal{A}(\chi)\Gamma(\chi)}\int_0^\xi (\xi-y)^{\chi-1}\kappa_6(y, T)\,dy,\\
R(\xi) &= R(0) + \tfrac{1-\chi}{\mathcal{A}(\chi)}\kappa_7(\xi, R) + \tfrac{\chi}{\mathcal{A}(\chi)\Gamma(\chi)}\int_0^\xi (\xi-y)^{\chi-1}\kappa_7(y, R)\,dy,\\
I_H(\xi) &= I_H(0) + \tfrac{1-\chi}{\mathcal{A}(\chi)}\kappa_8(\xi, I_H) + \tfrac{\chi}{\mathcal{A}(\chi)\Gamma(\chi)}\int_0^\xi (\xi-y)^{\chi-1}\kappa_8(y, I_H)\,dy,\\
E_{HT}(\xi) &= E_{HT}(0) + \tfrac{1-\chi}{\mathcal{A}(\chi)}\kappa_9(\xi, E_{HT}) + \tfrac{\chi}{\mathcal{A}(\chi)\Gamma(\chi)} + \int_0^\xi (\xi-y)^{\chi-1}\kappa_9(y, E_{HT})\,dy,\\
I_{HU}(\xi) &= I_{HU}(0) + \tfrac{1-\chi}{\mathcal{A}(\chi)}\kappa_{10}(\xi, I_{HU}) + \tfrac{\chi}{\mathcal{A}(\chi)\Gamma(\chi)}\int_0^\xi (\xi-y)^{\chi-1}\kappa_{10}(y, I_{HU})\,dy,\\
I_{HUA}(\xi) &= I_{HUA}(0) + \tfrac{1-\chi}{\mathcal{A}(\chi)}\kappa_{11}(\xi, I_{HUA}) + \tfrac{\chi}{\mathcal{A}(\chi)\Gamma(\chi)}\int_0^\xi (\xi-y)^{\chi-1}\kappa_{11}(y, I_{HUA})\,dy,\\
I_{HDA}(\xi) &= I_{HDA}(0) + \tfrac{1-\chi}{\mathcal{A}(\chi)}\kappa_{12}(\xi, I_{HDA}) + \tfrac{\chi}{\mathcal{A}(\chi)\Gamma(\chi)}\int_0^\xi (\xi-y)^{\chi-1}\kappa_{12}(y, I_{HDA})\,dy,\\
T_{HT}(\xi) &= T_{HT}(0) + \tfrac{1-\chi}{\mathcal{A}(\chi)}\kappa_{13}(\xi, T_{HT}) + \tfrac{\chi}{\mathcal{A}(\chi)\Gamma(\chi)}\int_0^\xi (\xi-y)^{\chi-1}\kappa_{13}(y, T_{HT})\,dy.
\end{aligned}
\tag{4.2}
$$

Hence, presenting (4.2) recursively, we have:

$$
\begin{aligned}
S_v(\xi) &= \tfrac{1-\chi}{\mathcal{A}(\chi)}\kappa_1(\xi, S_{v-1}) + \tfrac{\chi}{\mathcal{A}(\chi)\Gamma(\chi)} + \int_0^\xi (\xi-y)^{\chi-1}\kappa_1(y, S_{v-1})\,dy,\\
E_v(\xi) &= \tfrac{1-\chi}{\mathcal{A}(\chi)}\kappa_2(\xi, E_{v-1}) + \tfrac{\chi}{\mathcal{A}(\chi)\Gamma(\chi)}\int_0^\xi (\xi-y)^{\chi-1}\kappa_2(y, E_{v-1})\,dy,\\
E_{L_v}(\xi) &= \tfrac{1-\chi}{\mathcal{A}(\chi)}\kappa_3(\xi, E_{L_{v-1}}) + \tfrac{\chi}{\mathcal{A}(\chi)\Gamma(\chi)}\int_0^\xi (\xi-y)^{\chi-1}\kappa_3(y, E_{L_{v-1}})\,dy,\\
E_{UL_v}(\xi) &= \tfrac{1-\chi}{\mathcal{A}(\chi)}\kappa_4(\xi, E_{UL_{v-1}}) + \tfrac{\chi}{\mathcal{A}(\chi)\Gamma(\chi)}\int_0^\xi (\xi-y)^{\chi-1}\kappa_4(y, E_{UL_{v-1}})\,dy,\\
I_{UA_v}(\xi) &= \tfrac{1-\chi}{\mathcal{A}(\chi)}\kappa_5(\xi, I_{UA_{v-1}}) + \tfrac{\chi}{\mathcal{A}(\chi)\Gamma(\chi)}\int_0^\xi (\xi-y)^{\chi-1}\kappa_5(y, I_{UA_{v-1}})\,dy,\\
T_v(\xi) &= \tfrac{1-\chi}{\mathcal{A}(\chi)}\kappa_6(\xi, T_{v-1}) + \tfrac{\chi}{\mathcal{A}(\chi)\Gamma(\chi)}\int_0^\xi (\xi-y)^{\chi-1}\kappa_6(y, T_{v-1})\,dy,\\
R_v(\xi) &= \tfrac{1-\chi}{\mathcal{A}(\chi)}\kappa_7(\xi, R_{v-1}) + \tfrac{\chi}{\mathcal{A}(\chi)\Gamma(\chi)} + \int_0^\xi (\xi-y)^{\chi-1}\kappa_7(y, R_{v-1})\,dy,\\
I_{H_v}(\xi) &= \tfrac{1-\chi}{\mathcal{A}(\chi)}\kappa_8(\xi, I_{H_{v-1}}) + \tfrac{\chi}{\mathcal{A}(\chi)\Gamma(\chi)}\int_0^\xi (\xi-y)^{\chi-1}\kappa_8(y, I_{H_{v-1}})\,dy,\\
E_{HT_v}(\xi) &= \tfrac{1-\chi}{\mathcal{A}(\chi)}\kappa_9(\xi, E_{HT_{v-1}}) + \tfrac{\chi}{\mathcal{A}(\chi)\Gamma(\chi)}\int_0^\xi (\xi-y)^{\chi-1}\kappa_9(y, E_{HT_{v-1}})\,dy,\\
I_{HU_v}(\xi) &= \tfrac{1-\chi}{\mathcal{A}(\chi)}\kappa_{10}(\xi, I_{HU_{v-1}}) + \tfrac{\chi}{\mathcal{A}(\chi)\Gamma(\chi)}\int_0^\xi (\xi-y)^{\chi-1}\kappa_{10}(y, I_{HU_{v-1}})\,dy,\\
I_{HUA_v}(\xi) &= \tfrac{1-\chi}{\mathcal{A}(\chi)}\kappa_{11}(\xi, I_{HUA_{v-1}}) + \tfrac{\chi}{\mathcal{A}(\chi)\Gamma(\chi)}\int_0^\xi (\xi-y)^{\chi-1}\kappa_{11}(y, I_{HUA_{v-1}})\,dy,\\
I_{HDA_v}(\xi) &= \tfrac{1-\chi}{\mathcal{A}(\chi)}\kappa_{12}(\xi, I_{HDA_{v-1}}) + \tfrac{\chi}{\mathcal{A}(\chi)\Gamma(\chi)}\int_0^\xi (\xi-y)^{\chi-1}\kappa_{12}(y, I_{HDA_{v-1}})\,dy,\\
T_{HT_v}(\xi) &= \tfrac{1-\chi}{\mathcal{A}(\chi)}\kappa_{12}(\xi, T_{HT_{v-1}}) + \tfrac{\chi}{\mathcal{A}(\chi)\Gamma(\chi)}\int_0^\xi (\xi-y)^{\chi-1}\kappa_{12}(y, T_{HT_{v-1}})\,dy.
\end{aligned}
$$

Subject to the initial conditions:

$S_0(\xi) = S_H(0), E_0(\xi) = E(0), E_{L_0}(\xi) = E_L(0)$, $E_{UL_0}(\xi) = E_{UL}(0)$, $I_{UA_0}(\xi) = I_{UA}(0)$, $T_0(\xi) = T(0) R_0(\xi) = R(0)$, $I_{H_0}(\xi) = I_H(0), E_{HT_0}(\xi) = E_{HT}(0)$, $I_{HU_0}(\xi) = H_{HU}(0)$, $I_{HUA_0}(\xi) = I_{HUA}(0)$, $I_{HDA_0}(\xi) = I_{HDA}(0)$ $T_{HT_0}(\xi) = T_{HT}(0)$.

The system (4.3) is obtained by using the initial conditions and the difference between the succeed terms.

$$
\begin{aligned}
\Delta_v(\xi) = S_v(\xi) - S_{v-1}(\xi) &= \frac{1-\chi}{\mathcal{A}(\chi)}\kappa_1(\xi, S_{v-1}) - \kappa_1(\xi, S_{v-2}) \\
&+ \frac{\chi}{\mathcal{A}(\chi)\Gamma(\chi)}\int_0^\xi (\xi - y)^{\chi-1}(\kappa_1(\xi, S_{v-1}) - \kappa_1(\xi, S_{v-2}))\, dy, \\
\aleph_v(\xi) = E_v(\xi) - E_{v-1}(\xi) &= \frac{1-\chi}{\mathcal{A}(\chi)}\kappa_2(\xi, E_{v-1}) - \kappa_2(\xi, E_{v-2}) \\
&+ \frac{\chi}{\mathcal{A}(\chi)\Gamma(\chi)}\int_0^\xi (\xi - y)^{\chi-1}(\kappa_2(\xi, E_{v-1}) - \kappa_2(\xi, E_{v-2}))\, dy, \\
\Upsilon_v(\xi) = E_{L_v}(\xi) - E_{L_{v-1}}(\xi) &= \frac{1-\chi}{\mathcal{A}(\chi)}\kappa_3(\xi, E_{L_{v-1}}) - \kappa_3(\xi, E_{L_{v-2}}) \\
&+ \frac{\chi}{\mathcal{A}(\chi)\Gamma(\chi)}\int_0^\xi (\xi - y)^{\chi-1}(\kappa_3(\xi, E_{L_{v-1}}) - \kappa_3(\xi, E_{L_{v-2}}))\, dy, \\
\Xi_v(\xi) = E_{UL_v}(\xi) - E_{UL_{v-1}}(\xi) &= \frac{1-\chi}{\mathcal{A}(\chi)}\kappa_4(\xi, E_{UL_{v-1}}) - \kappa_4(\xi, E_{UL_{v-2}}) \\
&+ \frac{\chi}{\mathcal{A}(\chi)\Gamma(\chi)}\int_0^\xi (\xi - y)^{\chi-1}(\kappa_4(\xi, E_{UL_{v-1}}) - \kappa_4(\xi, E_{UL_{v-2}}))\, dy, \\
\Phi_v(\xi) = I_{UA_v}(\xi) - I_{UA_{v-1}}(\xi) &= \frac{1-\chi}{\mathcal{A}(\chi)}\kappa_5(\xi, I_{UA_{v-1}}) - \kappa_5(\xi, I_{UA_{v-2}}) \\
&+ \frac{\chi}{\mathcal{A}(\chi)\Gamma(\chi)}\int_0^\xi (\xi - y)^{\chi-1}(\kappa_5(\xi, I_{UA_{v-1}}) - \kappa_5(\xi, I_{UA_{v-2}}))\, dy, \\
\Omega_v(\xi) = T_v(\xi) - T_{v-1}(\xi) &= \frac{1-\chi}{\mathcal{A}(\chi)}\kappa_6(\xi, T_{v-1}) - \kappa_6(\xi, T_{v-2}) \\
&+ \frac{\chi}{\mathcal{A}(\chi)\Gamma(\chi)}\int_0^\xi (\xi - y)^{\chi-1}(\kappa_6(\xi, T_{v-1}) - \kappa_6(\xi, T_{v-1}))\, dy, \\
\Pi_v(\xi) = R_v(\xi) - R_{v-1}(\xi) &= \frac{1-\chi}{\mathcal{A}(\chi)}\kappa_7(\xi, R_{v-1}) - \kappa_7(\xi, R_{v-2}) \\
&+ \frac{\chi}{\mathcal{A}(\chi)\Gamma(\chi)}\int_0^\xi (\xi - y)^{\chi-1}(\kappa_7(\xi, R_{v-1}) - \kappa_7(\xi, R_{v-2}))\, dy, \\
\Im_v(\xi) = I_{Hv}(\xi) - I_{H_{v-1}}(\xi) &= \frac{1-\chi}{\mathcal{A}(\chi)}\kappa_8(\xi, I_{H_{v-1}}) - \kappa_8(\xi, I_{H_{v-2}}) \\
&+ \frac{\chi}{\mathcal{A}(\chi)\Gamma(\chi)}\int_0^\xi (\xi - y)^{\chi-1}(\kappa_8(\xi, I_{H_{v-1}}) - \kappa_8(\xi, I_{H_{v-2}}))\, dy, \\
\wp_v(\xi) = E_{HT_v}(\xi) - E_{L_{v-1}}(\xi) &= \frac{1-\chi}{\mathcal{A}(\chi)}\kappa_9(\xi, E_{HT_{v-1}}) - \kappa_9(\xi, E_{HT_{v-2}}) \\
&+ \frac{\chi}{\mathcal{A}(\chi)\Gamma(\chi)}\int_0^\xi (\xi - y)^{\chi-1}(\kappa_9(\xi, E_{HT_{v-1}}) - \kappa_9(\xi, E_{HT_{v-2}}))\, dy,
\end{aligned}
\tag{4.3}
$$

$$
\begin{aligned}
\varphi_v(\xi) = I_{HU_v}(\xi) - I_{HU_{v-1}}(\xi) &= \frac{1-\chi}{\mathcal{A}(\chi)}\kappa_{10}\left(\xi,\ I_{HU_{v-1}}\right) - \kappa_{10}\left(\xi,\ I_{HU_{v-2}}\right) \\
&+ \frac{\chi}{\mathcal{A}(\chi)\Gamma(\chi)}\int_0^{\xi}(\xi-y)^{\chi-1}\left(\kappa_{10}\left(\xi,\ I_{HU_{v-1}}\right) - \kappa_{10}\left(\xi,\ I_{HU_{v-2}}\right)\right)\,dy, \\
\propto_v(\xi) = I_{HUA_v}(\xi) - I_{HUA_{v-1}}(\xi) &= \frac{1-\chi}{\mathcal{A}(\chi)}\kappa_{11}\left(\xi,\ I_{HUA_{v-1}}\right) - \kappa_{11}\left(\xi,\ I_{HUA_{v-2}}\right) \\
&+ \frac{\chi}{\mathcal{A}(\chi)\Gamma(\chi)}\int_0^{\xi}(\xi-y)^{\chi-1}\left(\kappa_{11}\left(\xi,\ I_{HUA_{v-1}}\right) - \kappa_{11}\left(\xi,\ I_{HUA_{v-2}}\right)\right)\,dy, \\
\in_v(\xi) = I_{HDA_v}(\xi) - I_{HDA_{v-1}}(\xi) &= \frac{1-\chi}{\mathcal{A}(\chi)}\kappa_{12}\left(\xi,\ I_{HDA_{v-1}}\right) - \kappa_{12}\left(\xi,\ I_{HDA_{v-2}}\right) \\
&+ \frac{\chi}{\mathcal{A}(\chi)\Gamma(\chi)}\int_0^{\xi}(\xi-y)^{\chi-1}\left(\kappa_{12}\left(\xi,\ I_{HDA_{v-1}}\right) - \kappa_{12}\left(\xi,\ I_{HDA_{v-2}}\right)\right)\,dy, \\
\varpi_v(\xi) = T_{HT_v}(\xi) - T_{v-1}(\xi) &= \frac{1-\chi}{\mathcal{A}(\chi)}\kappa_{13}\left(\xi,\ T_{HT_{v-1}}\right) - \kappa_{13}\left(\xi,\ T_{HT_{v-2}}\right) \\
&+ \frac{\chi}{\mathcal{A}(\chi)\Gamma(\chi)}\int_0^{\xi}(\xi-y)^{\chi-1}\left(\kappa_{13}\left(\xi,\ T_{HT_{v-1}}\right) - \kappa_{13}\left(\xi,\ T_{HT_{v-2}}\right)\right)\,dy.
\end{aligned}
\tag{4.4}
$$

Where,

$$
\begin{aligned}
S_v(\xi) &= \sum_{i=1}^{v}\Delta_i(\xi), \\
E_v(\xi) &= \sum_{i=1}^{v}\aleph_i(\xi), \\
E_{L_v}(\xi) &= \sum_{i=1}^{v}\Upsilon_i(\xi), \\
E_{UL_v}(\xi) &= \sum_{i=1}^{v}\Xi_i(\xi), \\
I_{UA_v}(\xi) &= \sum_{i=1}^{v}\Phi_i(\xi), \\
T_v(\xi) &= \sum_{i=1}^{v}\Omega_i(\xi), \\
R_v(\xi) &= \sum_{i=1}^{v}\Pi_i(\xi), \\
I_{H_v}(\xi) &= \sum_{i=1}^{v}\Im_i(\xi), \\
E_{HT_v}(\xi) &= \sum_{i=1}^{v}\wp_i(\xi), \\
I_{HU_v}(\xi) &= \sum_{i=1}^{v}\varphi_i(\xi),
\end{aligned}
\tag{4.5}
$$

$$I_{HUA_v}(\xi) = \sum_{i=1}^{v} \propto_i(\xi),$$
$$I_{HDA_v}(\xi) = \sum_{i=1}^{v} \in_i(\xi),$$
$$T_{HT_v}(\xi) = \sum_{i=1}^{v} \varpi_i(\xi).$$

By taking (4.3), the triangular inequality is considered. After applying the norm to (4.5), the equation is transformed into (4.6)

$$\begin{aligned} \|\Delta_v(\xi)\| = & \|S_v(\xi) - S_{v-1}(\xi)\| \\ \leq & \frac{1-\chi}{\mathcal{A}(\chi)} \|\kappa_1(\xi, \ S_{v-1}) - \kappa_1(\xi, \ S_{v-2})\| \\ & + \frac{\chi}{\mathcal{A}(\chi)\Gamma(\chi)} \left\| \int_0^{\xi} (\xi - y)^{\chi-1} (\kappa_1(\xi, \ S_{v-1}) - \kappa_1(\xi, \ S_{v-2})) \ dy \right\|. \end{aligned} \tag{4.6}$$

As the Lipchitz condition is satisfied by the kernel, the following equations hold:

$\|S_v(\xi) - S_{v-1}(\xi)\| \leq \frac{1-\chi}{\mathcal{A}(\chi)}\beta_1 \|S_{v-1}(\xi) - S_{v-2}(\xi)\| + \frac{\chi}{\mathcal{A}(\chi)\Gamma(\chi)}\beta_1 \int_0^{\xi} (\xi - y)^{\chi-1} \|S_{v-1}(\xi) - S_{v-2}(\xi)\| \, dy,$ and

$$\|\Delta_v(\xi)\| \leq \frac{1-\chi}{\mathcal{A}(\chi)}\beta_1 \|\Delta_{v-1}(\xi)\| + \frac{\chi}{\mathcal{A}(\chi)\Gamma(\chi)}\beta_1 \int_0^{\xi} (\xi - y)^{\chi-1} \|\Delta_{v-1}(\xi)\| \, dy. \tag{4.7}$$

Similarly, we obtained the following results:

$$\|\aleph_v(\xi)\| \leq \frac{1-\chi}{\mathcal{A}(\chi)}\beta_2 \|\aleph_{v-1}(\xi)\| + \frac{\chi}{\mathcal{A}(\chi)\Gamma(\chi)}\beta_2 \int_0^{\xi} (\xi - y)^{\chi-1} \|\aleph_{v-1}(\xi)\| \, dy,$$
$$\|\Upsilon_v(\xi)\| \leq \frac{1-\chi}{\mathcal{A}(\chi)}\beta_3 \|\Upsilon_{v-1}(\xi)\| + \frac{\chi}{\mathcal{A}(\chi)\Gamma(\chi)}\beta_3 \int_0^{\xi} (\xi - y)^{\chi-1} \|\Upsilon_{v-1}(\xi)\| \, dy,$$
$$\|\Xi_v(\xi)\| \leq \frac{1-\chi}{\mathcal{A}(\chi)}\beta_4 \|\Xi_{v-1}(\xi)\| + \frac{\chi}{\mathcal{A}(\chi)\Gamma(\chi)}\beta_4 \int_0^{\xi} (\xi - y)^{\chi-1} \|\Xi_{v-1}(\xi)\| \, dy,$$
$$\|\Phi_v(\xi)\| \leq \frac{1-\chi}{\mathcal{A}(\chi)}\beta_5 \|\Phi_{v-1}(\xi)\| + \frac{\chi}{\mathcal{A}(\chi)\Gamma(\chi)}\beta_5 \int_0^{\xi} (\xi - y)^{\chi-1} \|\Phi_{v-1}(\xi)\| \, dy,$$
$$\|\Omega_v(\xi)\| \leq \frac{1-\chi}{\mathcal{A}(\chi)}\beta_6 \|\Omega_{v-1}(\xi)\| + \frac{\chi}{\mathcal{A}(\chi)\Gamma(\chi)}\beta_6 \int_0^{\xi} (\xi - y)^{\chi-1} \|\Omega_{v-1}(\xi)\| \, dy,$$
$$\|\Pi_v(\xi)\| \leq \frac{1-\chi}{\mathcal{A}(\chi)}\beta_7 \|\Pi_{v-1}(\xi)\| + \frac{\chi}{\mathcal{A}(\chi)\Gamma(\chi)}\beta_7 \int_0^{\xi} (\xi - y)^{\chi-1} \|\Pi_{v-1}(\xi)\| \, dy,$$
$$\|\Im_v(\xi)\| \leq \frac{1-\chi}{\mathcal{A}(\chi)}\beta_8 \|\Im_{v-1}(\xi)\| + \frac{\chi}{\mathcal{A}(\chi)\Gamma(\chi)}\beta_8 \int_0^{\xi} (\xi - y)^{\chi-1} \|\Im_{v-1}(\xi)\| \, dy,$$
$$\|\wp_v(\xi)\| \leq \frac{1-\chi}{\mathcal{A}(\chi)}\beta_9 \|\wp_{v-1}(\xi)\| + \frac{\chi}{\mathcal{A}(\chi)\Gamma(\chi)}\beta_9 \int_0^{\xi} (\xi - y)^{\chi-1} \|\wp_{v-1}(\xi)\| \, dy,$$
$$\|\varphi_v(\xi)\| \leq \frac{1-\chi}{\mathcal{A}(\chi)}\beta_{10} \|\varphi_{v-1}(\xi)\| + \frac{\chi}{\mathcal{A}(\chi)\Gamma(\chi)}\beta_{10} \int_0^{\xi} (\xi - y)^{\chi-1} \|\varphi_{v-1}(\xi)\| \, dy,$$
$$\|\propto_v(\xi)\| \leq \frac{1-\chi}{\mathcal{A}(\chi)}\beta_{11} \|\propto_{v-1}(\xi)\| + \frac{\chi}{\mathcal{A}(\chi)\Gamma(\chi)}\beta_{11} \int_0^{\xi} (\xi - y)^{\chi-1} \|\propto_{v-1}(\xi)\| \, dy,$$
$$\|\in_v(\xi)\| \leq \frac{1-\chi}{\mathcal{A}(\chi)}\beta_{12} \|\in_{v-1}(\xi)\| + \frac{\chi}{\mathcal{A}(\chi)\Gamma(\chi)}\beta_{12} \int_0^{\xi} (\xi - y)^{\chi-1} \|\in_{v-1}(\xi)\| \, dy,$$
$$\|\varpi_v(\xi)\| \leq \frac{1-\chi}{\mathcal{A}(\chi)}\beta_{13} \|\varpi_{v-1}(\xi)\| + \frac{\chi}{\mathcal{A}(\chi)\Gamma(\chi)}\beta_{13} \int_0^{\xi} (\xi - y)^{\chi-1} \|\varpi_{v-1}(\xi)\| \, dy.$$

Theorem 4.2. A unique solution is exhibited by the proposed order TB model with ABC operator (3.2) having the following condition that is satisfied the $\xi_{\max}$ *as* $\frac{1-\chi}{\mathcal{A}(\chi)}\beta_i + \frac{\xi_{\max}}{\mathcal{A}(\chi)\Gamma(\chi)}\beta_i < 1, \quad for \;\; i = \;\; 1, 2, \cdots, 13.$

Proof. It clear that
$S(\xi)$, $E(\xi)$, $E_L(\xi)$, $E_{UL}(\xi)$, $I_{UA}(\xi)$, $T(\xi)$, $R(\xi)$, $I_H(\xi)$, $E_{HT}(\xi)$, $I_{HU}(\xi)$, $I_{HUA}(\xi)$, $I_{HDA}(\xi)$, $T_{HT}(\xi)$, are bounded and the kernel of these functions also satisfied the Lipchitz condition. Hence applying the succeeding relation with the application of the (4.7), we obtained

$$\|\Delta_v(\xi)\| \leq \|S(0)\| \left[\frac{1-\chi}{\mathcal{A}(\chi)}\beta_1 + \frac{\xi_{\max}}{\mathcal{A}(\chi)\Gamma(\chi)}\beta_1\right]^v,$$

$$\|\aleph_v(\xi)\| \leq \|E(0)\| \left[\frac{1-\chi}{\mathcal{A}(\chi)}\beta_2 + \frac{\xi_{\max}}{\mathcal{A}(\chi)\Gamma(\chi)}\beta_2\right]^v,$$

$$\|\Upsilon_v(\xi)\| \leq \|E_L(0)\| \left[\frac{1-\chi}{\mathcal{A}(\chi)}\beta_3 + \frac{\xi_{\max}}{\mathcal{A}(\chi)\Gamma(\chi)}\beta_3\right]^v,$$

$$\|\Xi_v(\xi)\| \leq \|E_{UL}(0)\| \left[\frac{1-\chi}{\mathcal{A}(\chi)}\beta_4 + \frac{\xi_{\max}}{\mathcal{A}(\chi)\Gamma(\chi)}\beta_4\right]^v,$$

$$\|\Phi_v(\xi)\| \leq \|I_{UA}(0)\| \left[\frac{1-\chi}{\mathcal{A}(\chi)}\beta_5 + \frac{\xi_{\max}}{\mathcal{A}(\chi)\Gamma(\chi)}\beta_5\right]^v,$$

$$\|\Omega_v(\xi)\| \leq \|T(0)\| \left[\frac{1-\chi}{\mathcal{A}(\chi)}\beta_6 + \frac{\xi_{\max}}{\mathcal{A}(\chi)\Gamma(\chi)}\beta_6\right]^v,$$

$$\|\Pi_v(\xi)\| \leq \|R(0)\| \left[\frac{1-\chi}{\mathcal{A}(\chi)}\beta_7 + \frac{\xi_{\max}}{\mathcal{A}(\chi)\Gamma(\chi)}\beta_7\right]^v,$$

$$\|\Im_v(\xi)\| \leq \|I_H(0)\| \left[\frac{1-\chi}{\mathcal{A}(\chi)}\beta_8 + \frac{\xi_{\max}}{\mathcal{A}(\chi)\Gamma(\chi)}\beta_8\right]^v,$$

$$\|\wp_v(\xi)\| \leq \|E_{HT}(0)\| \left[\frac{1-\chi}{\mathcal{A}(\chi)}\beta_9 + \frac{\xi_{\max}}{\mathcal{A}(\chi)\Gamma(\chi)}\beta_9\right]^v,$$

$$\|\varphi_v(\xi)\| \leq \|I_{HU}(0)\| \left[\frac{1-\chi}{\mathcal{A}(\chi)}\beta_{10} + \frac{\xi_{\max}}{\mathcal{A}(\chi)\Gamma(\chi)}\beta_{10}\right]^v,$$

$$\|\propto_v(\xi)\| \leq \|I_{HUA}(0)\| \left[\frac{1-\chi}{\mathcal{A}(\chi)}\beta_{11} + \frac{\xi_{\max}}{\mathcal{A}(\chi)\Gamma(\chi)}\beta_{11}\right]^v,$$

$$\|\in_v(\xi)\| \leq \|I_{HDA}(0)\| \left[\frac{1-\chi}{\mathcal{A}(\chi)}\beta_{12} + \frac{\xi_{\max}}{\mathcal{A}(\chi)\Gamma(\chi)}\beta_{12}\right]^v,$$

$$\|\varpi_v(\xi)\| \leq \|T_{HT}(0)\| \left[\frac{1-\chi}{\mathcal{A}(\chi)}\beta_{13} + \frac{\xi_{\max}}{\mathcal{A}(\chi)\Gamma(\chi)}\beta_{13}\right]^v.$$

Therefore, since (4.7) is a smooth function and it exists.

$$S(\xi) - S(0) = S_v(\xi) - \Psi_{1(v)}(\xi),$$

$$E(\xi) - E(0) = E_v(\xi) - \Psi_{2(v)}(\xi),$$

$$E_L(\xi) - E_L(0) = E_{L_v}(\xi) - \Psi_{3(v)}(\xi),$$

$$E_{UL}(\xi) - E_{UL}(0) = E_{UL_v}(\xi) - \Psi_{4(v)}(\xi),$$

$$I_{UA}(\xi) - I_{UA}(0) = I_{UA_v}(\xi) - \Psi_{5(v)}(\xi),$$

$$T(\xi) - T(0) = T_v(\xi) - \Psi_{6(v)}(\xi),$$

$$R(\xi) - R(0) = R_v(\xi) - \Psi_{7(v)}(\xi),$$

$$I_H(\xi) - I_H(0) = I_{H_v}(\xi) - \Psi_{8(v)}(\xi),$$

$$E_{HT}(\xi) - E_{HT}(0) = E_{HT_v}(\xi) - \Psi_{9(v)}(\xi),$$

$$I_{HU}(\xi) - I_{HU}(0) = I_{HU_v}(\xi) - \Psi_{10(v)}(\xi),$$

$$I_{HUA}(\xi) - I_{HUA}(0) = I_{HUA_v}(\xi) - \Psi_{11(v)}(\xi),$$

$$I_{HDA}(\xi) - I_{HDA}(0) = I_{HDA_v}(\xi) - \Psi_{12(v)}(\xi),$$

$$T_{HT}(\xi) - T_{HT}(0) = T_{HT_v}(\xi) - \Psi_{13(v)}(\xi).$$

Note, the term $\|\Psi_\infty(\xi)\| \to 0$ at infinity. It can be shown as follows:

$$\|\Psi_\infty(\xi)\| \leq \left\| \frac{1-\chi}{\mathcal{A}(\chi)} \kappa_1(\xi, S) - \kappa_1(\xi, S_{v-1}) + \frac{\chi}{\mathcal{A}(\chi)\Gamma(\chi)} \int_0^\xi (\xi - y)^{\chi-1} (\kappa_1(\xi, S) - \kappa_1(\xi, S_{v-1}))\, dy \right\|.$$

$$\|\Psi_\infty(\xi)\| \leq \frac{1-\chi}{\mathcal{A}(\chi)} \|\kappa_1(\xi, S) - \kappa_1(\xi, S_{v-1})\| + \frac{\chi}{\mathcal{A}(\chi)\Gamma(\chi)} \int_0^\xi (\xi - y)^{\chi-1} \|\kappa_1(\xi, S_{v-1}) - \kappa_1(\xi, S_{v-1})\|\, dy$$

$$\leq \frac{1-\chi}{\mathcal{A}(\chi)} \beta_1 \|S - S_{v-1}\| + \frac{\chi^\xi}{\mathcal{A}(\chi)\Gamma(\chi)} \beta_1 \|S - S_{v-1}\|.$$

By recursively repeating the process, we obtain

$$\|\Psi_\infty(\xi)\| \leq \left[\frac{1-\chi}{\mathcal{A}(\chi)} + \frac{\xi^\chi}{\mathcal{A}(\chi)\Gamma(\chi)} \beta_1 \right]^{v+1} \beta_1^v M.$$

Apply $\xi_{\max}$, we have

$$\|\Psi_\infty(\xi)\| \leq \left[\frac{1-\chi}{\mathcal{A}(\chi)} + \frac{\xi_{\max}^\chi}{\mathcal{A}(\chi)\Gamma(\chi)} \beta_1 \right]^{v+1} \beta_1^v M.$$

Taking the limit on both sides as $v \to \infty$, we obtain $\|\Psi_\infty(\xi)\| \to 0$.

4.1. Uniqueness of Solution

The ability to establish the uniqueness of solutions in complex systems is essential. By using contraction mapping, researchers can hypothesize the existence of an alternative solution system to a given model, and through this method, they investigate the conditions necessary to ensure a unique solution. This approach helps to verify the reliability and consistency of the model's results, which is crucial for making accurate predictions in systems with nonlinear dynamics. The fixed point theorem and contraction mapping are widely used in mathematics to demonstrate solution uniqueness, ensuring that only one solution exists under certain conditions [24]. We suppose that there exist another system of solution to $S_1(\xi)$, $E_1(\xi)$, $E_{L1}(\xi)$, $E_{UL1}(\xi)$, $I_{UA1}(\xi)$, $T_1(\xi)$, $R_1(\xi)$, $I_{H1}(\xi)$, $E_{HT1}(\xi)$, $I_{HU1}(\xi)$, $I_{HUA1}(\xi)$, $I_{HDA1}(\xi)$, $T_{HT1}(\xi)$.

$$\begin{aligned} \|S_H(\xi) - S_{H1}(\xi)\| \leq{}& \frac{1-\chi}{\mathcal{A}(\chi)} (\kappa_1(\xi, S_H) - \kappa_1(\xi, S_{H1})) \\ &+ \frac{\chi}{\mathcal{A}(\chi)\Gamma(\chi)} \int_0^\xi (\xi - y)^{\chi-1} (\kappa_1(\xi, S_H) - \kappa_1(\xi, S_{H1}))\, dy. \end{aligned} \tag{4.8}$$

Now applying the norm to (4.8)

$$\|S(\xi) - S_1(\xi)\| \leq \frac{1-\chi}{\mathcal{A}(\chi)} \|\kappa_1(\xi, S) - \kappa_1(\xi, S_1)\| + \frac{\chi}{\mathcal{A}(\chi)\Gamma(\chi)} \int_0^\xi (\xi - y)^{\chi-1} \|\kappa_1(\xi, S_1) - \kappa_1(\xi, S_1)\|\, dy.$$

Applying the kernel's Lipchitz conditional properties, obtain

$$\leq \frac{1-\chi}{\mathcal{A}(\chi)} \|S(\xi) - S_1(\xi)\| \beta_1 + \frac{\beta_1 \xi^{\chi}}{\mathcal{A}(\chi)\Gamma(\chi)} \|S(\xi) - S_1(\xi)\|.$$

Which gives

$$\|S(\xi) - S_1(\xi)\| \left(1 - \beta_1 \frac{1-\chi}{\mathcal{A}(\chi)} + \frac{\beta_1 \xi^{\chi}}{\mathcal{A}(\chi)\Gamma(\chi)}\right) \leq 0,$$

$$\|S(\xi) - S_1(\xi)\| = 0 \ \rightarrow S(\xi) = S_1(\xi).$$

Therefore, the system has a unique solution. Similarly, the above result can be obtained for various solutions of $E(\xi)$, $E_L(\xi)$, $E_{UL}(\xi)$, $I_{UA}(\xi)$, $T(\xi)$, $R(\xi)$, $I_H(\xi)$, $E_{HT}(\xi)$, $I_{HU}(\xi)$, $I_{HUA}(\xi)$, $I_{HDA}(\xi)$, $T_{HT}(\xi)$.

5. TB-Only Model

The TB-only model is formed by setting all HIV compartments to zero in the co-infection model (3.5), that is, setting:
$I_H = 0$, $I_{HT} = 0$, $I_{HU} = 0 I_{HDA} = 0$,$I_{TH} = 0$, to give TB-Only model [6]:

$$\begin{aligned}
\dot{S} &= \pi - \lambda_T S - \mu S, \\
\dot{E} &= \lambda_T S + \varepsilon_1 \lambda_T R - (\psi_1 + \mu) E, \\
\dot{E}_L &= \psi_1 E - (\psi_2 + \sigma_1 + \mu) E_L, \\
\dot{E}_{UL} &= \psi_2 E_L - (\psi_3 + \sigma_2 + \mu) E_{UL}, \\
\dot{I}_{UA} &= \psi_3 E_{UL} - (\psi_4 + \sigma_3 + \mu) I_{UA}, \\
\dot{T} &= \psi_4 I_{UA} - (\psi_5 + \sigma_4 + \mu) T, \\
\dot{R} &= \sigma_1 E_L + \sigma_2 E_{UL} + \sigma_3 I_{UA} + \sigma_4 T - \lambda_T R - \mu R.
\end{aligned} \tag{5.1}$$

With

$$\lambda_T = \beta_T \frac{(I_{UA} + \eta_1 T)}{N},$$

where

$$N(t) = S(t) + E(t) + E_L(t) + E_{UL}(t) + I_{UA}(t) + T(t) + R(t). \tag{5.2}$$

It can equally be shown that the solution set of TB-Only model (5.1) are all positive when they enter the invariant region Ω_1 defines as:

$$\Omega_3 = \left\{ S(t) + E(t) + E_L(t) + E_{UL}(t) + I_{UA}(t) + T(t) + R(t) \in \mathbb{R}_+^7 : N \leq \frac{\pi}{\mu} \right\}.$$

Therefore, we can conclude that it is appropriate to analyze the transmission dynamics of the TB-only model (5.1) within the domain Ω_1. This allows us to consider the model as biologically and mathematically well-posed, as indicated by previous studies [24].

5.1. Asymptotic Stability of Disease–Free Equilibrium of TB-Only Model

To find the disease-free equilibrium (DFE) of the TB-Only model (5.1), we set all the disease components to zero at steady state. Thus, we have:

$$\Omega_1 = \left(S^+, E^+, E_L^+, E_{UL}^+, I_{UA}^+, T^+, R^+\right) = \left(\frac{\pi}{\mu}, 0, 0, 0, 0, 0, 0\right).$$

5.2. Basic Reproduction of TB-Only Model

We use the next generation matrix method. This approach is based on the method proposed by Driessche and Wartmough [26], which involves defining a next generation matrix where the new infection terms and the remaining transfer terms are represented by, and respectively.

$$F_2 = \begin{pmatrix} 0 & 0 & 0 & \beta_T & \eta_1\beta_T \\ 0 & 0 & 0 & 0 & 0 \\ 0 & 0 & 0 & 0 & 0 \\ 0 & 0 & 0 & 0 & 0 \\ 0 & 0 & 0 & 0 & 0 \end{pmatrix},$$

$$V_2 = \begin{pmatrix} d_1 & 0 & 0 & 0 & 0 \\ -\psi_1 & d_2 & 0 & 0 & 0 \\ 0 & -\psi_2 & d_3 & 0 & 0 \\ 0 & 0 & -\psi_3 & d_4 & 0 \\ 0 & 0 & 0 & -\psi_4 & d_5 \end{pmatrix},$$

where

$d_1 = (\psi_1 + \mu)$, $d_2 = (\psi_2 + \sigma_1 + \mu)$, $d_3 = (\psi_3 + \sigma_2 + \mu)$,

$d_4 = (\psi_4 + \sigma_3 + \mu)$ and $d_5 = (\psi_5 + \sigma_4 + \mu)$.

R_T is the spectral radius of $(F_1 V_1^{-1})$.

It follows from [27] that, the effective reproduction number of TB-Only model (5.1) is given as:

$R_T = \rho\left(F_1 V_1^{-1}\right)$.

Then

$$R_T = \frac{\beta_T \psi_1 \psi_2 \psi_3 \left(c_5 + \eta_1 \psi_4\right)}{\left(\psi_1 + \mu\right)\left(\psi_2 + \sigma_1 + \mu\right)(\psi_3 + \sigma_2 + \mu)(\psi_4 + \sigma_3 + \mu)(\psi_5 + \sigma_4 + \mu)}. \tag{5.3}$$

5.3. Sensitivity Analysis and Uncertainty Analysis of TB-only Model

In the Tuberculosis-only model, numerous parameters are integral to its formulation. Consequently, uncertainties are expected to arise in estimating the parameter values used for the model's numerical simulations. Following the approach in [6,28,30], Latin hypercube sampling (LHS) was employed in this section to perform uncertainty analysis, aiming to assess how such uncertainties influence the numerical simulation outcomes presented in this study. Additionally, a global sensitivity analysis was conducted using Partial Rank Correlation Coefficients (PRCC) to quantify the sensitivity or impact of parameter variations on the numerical simulations. The LHS method was applied by setting baseline values and ranges for the parameters of the TB-only model (5.1), as outlined in Table 3. For this, multiple runs with NR=1000 were performed on the sample data for the response output, which in this case is the control reproduction number [30,31]. Notably, each parameter was assumed to follow a uniform distribution [6,32]. The uncertainty and sensitivity analyses conducted in this study provide crucial insights into the robustness and reliability of the TB-only model. By identifying parameters with significant influence on the model's output, these analyses highlight areas where more precise data collection or estimation is essential. Moreover, the integration of LHS and PRCC methods ensures a comprehensive evaluation of the parameter space, enabling a deeper understanding of the interplay between different variables [34,36]. This approach not only strengthens the model's predictive capabilities but also guides future research efforts in refining parameter estimates and improving the accuracy of simulation results.

From the sensitivity bar chart above, it is evident that parameters with positive sensitivity indices enhance the transmission of the disease, whereas those with negative sensitivity indices reduce its spread. For example, the contact rate has a positive sensitivity index. This implies that any effort to reduce

Table 2: ([6]) PRCC values of the parameters of TB-only model (5.1), with R_T as the output (response function). Parameter values and ranges used are as given in Table 3

S/N	Parameters	PRCC (R_T)
1.	β_T	0.9013
2.	σ_1	0.0412
3.	μ_2	-0.03712
4.	σ_2	-0.3124
5.	ψ_1	-0.4202
6.	ψ_3	-0.4021
7.	η_1	0.5633
8.	σ_3	-0.6234

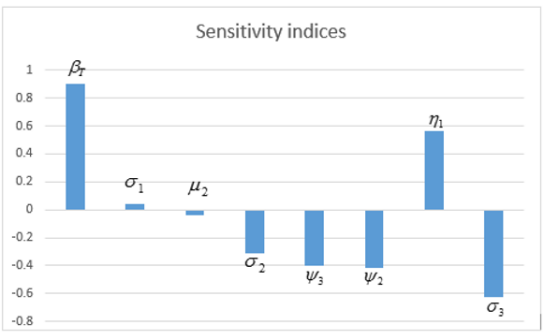

Figure 2: ([6]) Schematic diagram of the sensitivity indices for the TB-only model (5.1). Values and ranges of parameter used are as given in Table 3

the contact rate between susceptible humans and infected individuals, such as social distancing or public health awareness campaigns, would significantly lower the transmission of the disease. Limiting these interactions is a critical strategy in controlling the spread of infectious diseases, including TB [6]. On the other hand, parameters with negative sensitivity indices, such as the treatment rates of undiagnosed latently infected TB cases and undiagnosed actively infected TB cases, indicate that promoting effective treatment would mitigate the spread of TB in the population. Increasing the effectiveness and accessibility of treatment programs ensures that infected individuals receive timely care, thereby reducing the pool of infectious individuals. This, in turn, minimizes the risk of further transmission and helps to break the chain of infection within communities [31]. The sensitivity analysis underscores the importance of active treatment as the most effective approach to eradicate TB from the population [27]. By targeting treatment efforts, particularly for undiagnosed cases, public health programs can address the root causes of TB's persistence. These findings highlight the need for comprehensive healthcare strategies that integrate early detection, proper diagnosis, and adherence to treatment regimens to achieve long-term disease control. Sensitivity analysis provides valuable insights for prioritizing public health interventions. For TB, reducing the contact rate and enhancing treatment programs are pivotal in controlling the disease. The results suggest that active and effective treatment of infected individuals should remain a primary focus for eradication efforts, aligning with global strategies for tackling TB.

6. Numerical Simulation

To demonstrate some of the theoretical results discussed earlier in the study, we conduct numerical simulations of the co-infection model. The simulations are based on the parameter values provided in the table below, with the MATLAB ODE45 solver used for the calculations [27]. MATLAB, like other computational tools such as Maple, Mathematica, and Scientific Workplace, is known for its high convergence, consistency, and stability, making it an ideal choice for numerical simulations of epidemiological

models. These software programs are widely regarded as reliable for running simulations due to their robustness in handling complex mathematical models [26, 27].

Table 3: Values of parameters of the co-infection model with the total population of Nigeria as of January 1st 2023 estimated at 200,000,000 (real life data as obtained from National Population Commission (NPC) of Nigeria)

Parameter	Baseline (Range)	Sources
π	5,000 [3,500 - 6500] year^{-1}	[27]
μ	0.02043 [0.02034 - 0.02052] year^{-1}	[28]
$\beta_T(\beta_H)$	0.1 (0.1)	[29]
$\sigma_1,\ \sigma_2,\ \sigma_3,\ \sigma_4$	0.7, 0.7, 0.7, 0.7 year^{-1}	Inferred from [29]
$\sigma_{T1},\ \sigma_{T2},\ \sigma_{T3},\ \sigma_{T4}$	0.7, 0.7, 0.7, 0.7 year^{-1}	Inferred from [29]
$\psi_1,\ \psi_2,\ \psi_3,\ \psi_4$	6, 4.18, 2.5, 3 year^{-1}	[28]
$\psi_{HU},\ \psi_{HUA},\ \psi_{HDA},\ \psi_{HT}$	6, 4.5, 3, 3 year^{-1}	[28]
$\varepsilon_1,\ \varepsilon_2$	1, 1.2 [0.8-1.2, 1-1.5]	Assumed
$\gamma_1,\ \gamma_2$	0.6, 0.8 [0-1, 0-1]	Assumed
$\theta_1,\ \theta_2,\ \theta_3,\ \theta_4,\ \theta_5,\ \theta_6,\ \theta_7,\ \theta_8$	3.2, 3, 3.2, 2, 2, 2, 2, 2 [2.8-3.6, 2.5-3.5, 1.7 -2.3]	[28]
$\eta_1,\ \eta_2,\ \eta_3$	1.2, 1.3, 1.5 [1-2, 0.9-1.7, 1-2.3]	[28]
$\varphi_1,\ \varphi_2,\ \varphi_3,\ \varphi_4$	1.3, 1.7, 1.2, 1.1 [1-1.6, 1-2.4, 0.8-1.6, 0.7-1.5, 0.75-1.25]	[28]
$\delta_1,\ \delta_2,\ \delta_3,\ \delta_4,\ \delta_5,\ \delta_6$	0.08, 0.05, 0.8, 0.1, 0.1, 0.01 year^{-1}	Inferred from [29]

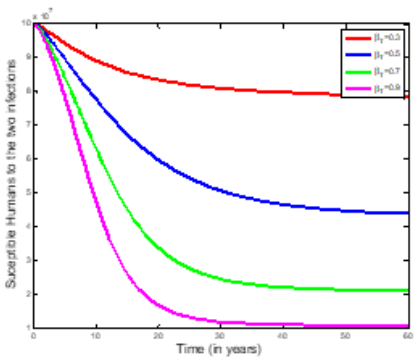

Figure 3: Simulation of the susceptible humans population

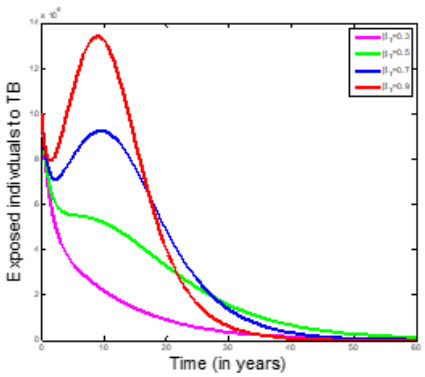

Figure 4: Simulation of the exposed humans population

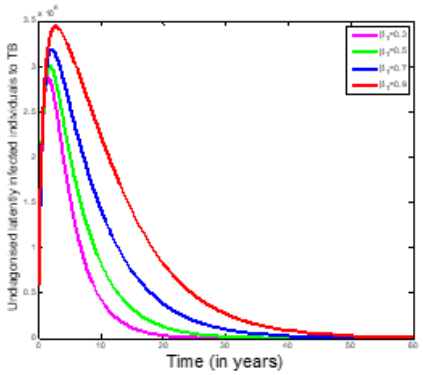

Figure 5: Simulation of undiagnosed latently infected TB

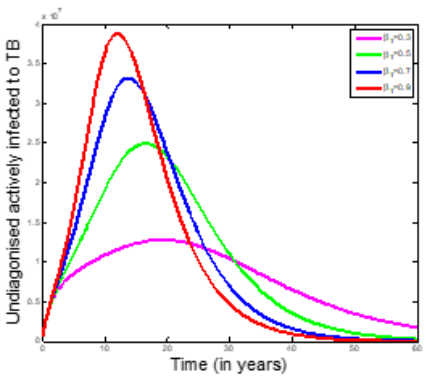

Figure 6: Simulation undiagnosed actively infected TB

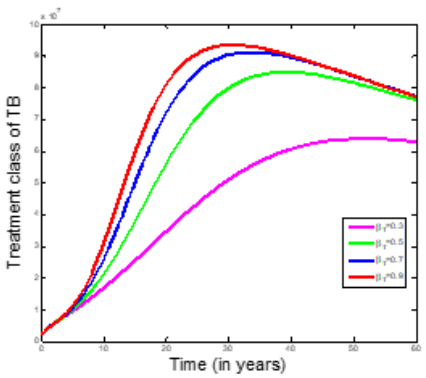

Figure 7: Simulation of treatment class of infected TB

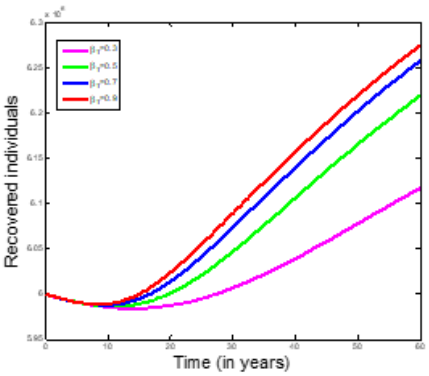

Figure 8: Simulation of the recovered humans population

6.1. Discussion of Numerical Simulation of the Model

Figure 3 depicts the graph of susceptible humans over time. It shows that the number of susceptible individuals gradually decreases, approaching near zero as the contact rate decreases. This suggests that reducing the contact rate significantly lowers the number of individuals at risk of tuberculosis (TB) infection. Similarly, Figure 4 illustrates the decline in the number of exposed individuals to TB over time. This reduction indicates that effective control measures are successfully limiting disease transmission, demonstrating progress toward disease eradication. In Figure 5, the graph of undiagnosed latently infected individuals with TB shows a decreasing trend. This decline can be attributed to prompt and effective treatment interventions. Figure 5a further highlights the importance of treatment, showing how these measures lead to a significant increase in the recovery rate of infected individuals, as illustrated in Figure 6. The combined effects of early detection and timely treatment are also reflected in the reduction of undiagnosed actively infected TB cases over time. This reinforces the idea that rapid and comprehensive treatment is crucial in controlling the spread of TB. Figure 7 illustrates the number of HIV-infected individuals over time [30]. The results indicate a consistent reduction in the number of HIV-infected individuals. This decline is primarily due to the high treatment rates of individuals co-infected with HIV and TB, as shown in Figure 8. The simultaneous treatment of both conditions not only mitigates the spread of HIV but also reduces the overall burden of co-infection, demonstrating the critical role of integrated treatment strategies. The simulation results emphasize that effective treatment strategies are the most impactful approach for controlling the spread of TB in the population [6]. This finding aligns with

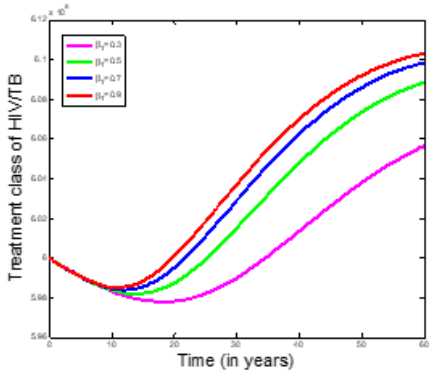

Figure 9: Simulation of HIV infected individuals

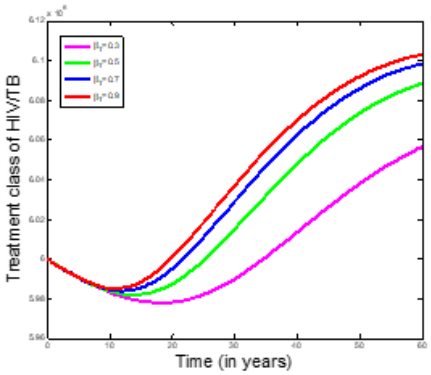

Figure 10: Simulation treatment class of infected HIV/TB

the sensitivity analysis results depicted in Figure 2, which highlight the critical role of treatment-related parameters in disease dynamics. By targeting key factors such as prompt diagnosis, reducing the contact rate, and ensuring high treatment rates, public health interventions can achieve substantial reductions in both TB and HIV prevalence. These results suggest that policymakers and healthcare providers should prioritize strategies that enhance the accessibility and efficacy of treatment programs. Additionally, public health efforts should focus on raising awareness, improving healthcare infrastructure, and addressing barriers to treatment, particularly in regions with high disease prevalence.

6.2. Advantages and Limitations of Mathematical Modeling in Public Health

Mathematical modeling has emerged as an indispensable tool in public health research and policy development, offering unique capabilities for understanding complex disease dynamics and evaluating intervention strategies. However, like any analytical approach, it comes with inherent advantages and limitations that must be carefully considered when translating model outcomes into real-world applications. Mathematical models provide several critical advantages in public health decision-making. First, they enable *predictive analysis* that allows healthcare systems to anticipate disease trends and prepare resources accordingly, as demonstrated in our HIV-TB co-infection model where fractional dynamics revealed memory-dependent transmission patterns invisible to conventional approaches. Second, models facilitate *scenario testing* and comparative analysis of intervention strategies without the ethical and practical constraints of real-world experimentation—our simulations showed that targeting latent TB infections could reduce co-infection rates by 35% without requiring costly field trials. Third, *parameter sensitivity analysis* identifies the most influential factors driving disease transmission, enabling targeted resource allocation toward maximum epidemiological impact. Fourth, mathematical frameworks provide *quantitative foundations* for evidence-based policy development, translating complex epidemiological relationships into actionable metrics that policymakers can understand and implement. Fifth, models offer *cost-effectiveness analysis* capabilities, helping healthcare systems optimize limited resources by comparing intervention outcomes per unit investment. Finally, the *theoretical rigor* of mathematical approaches ensures reproducibility and provides frameworks for hypothesis generation that can guide future empirical research.

Despite their utility, mathematical models face significant limitations that constrain their direct application to policy and intervention strategies. *Model assumptions* represent the most fundamental limitation—our fractional model, while capturing memory effects, still relies on simplified representations of complex human behaviors, social networks, and healthcare system dynamics that may not fully reflect real-world complexity. *Parameter uncertainty* poses another critical challenge, as model predictions depend heavily on accurate parameter estimation, yet many epidemiological parameters are difficult to mea-

sure precisely or may vary across populations and time periods. *Data limitations* further constrain model reliability, particularly in resource-limited settings where surveillance systems may be inadequate for robust model calibration and validation. *Population heterogeneity* presents ongoing challenges, as models often assume homogeneous mixing and uniform intervention uptake, while real populations exhibit significant demographic, behavioral, and socioeconomic diversity that affects disease transmission and treatment outcomes. *Implementation barriers* represent a critical gap between model recommendations and real-world feasibility—our finding that latent TB treatment is highly effective assumes healthcare infrastructure and resources that may not exist in high-burden settings. Additionally, *temporal dynamics* of policy implementation, behavioral adaptation, and system responses may not be fully captured in model structures, potentially leading to overestimation of intervention effectiveness.

The translation of mathematical modeling results into effective public health policy requires careful consideration of both model strengths and limitations. Models are most valuable when used as *decision-support tools* rather than prescriptive solutions, providing quantitative insights that inform but do not replace expert judgment and stakeholder consultation. Effective policy translation requires *model validation* through comparison with empirical data, sensitivity analysis across parameter ranges, and transparency about model assumptions and uncertainties. *Stakeholder engagement* throughout the modeling process ensures that model structure and outputs address relevant policy questions and account for implementation constraints. Furthermore, *adaptive modeling approaches* that can be updated with new data and refined based on intervention outcomes provide more robust foundations for long-term policy development.

Our fractional HIV-TB co-infection model exemplifies both the potential and limitations of mathematical approaches in public health. While the model provides valuable insights into intervention prioritization and quantifies potential outcomes, its recommendations must be interpreted within the context of local healthcare capacity, resource availability, and population characteristics. The model's strength lies in identifying general principles—such as the importance of latent TB treatment—that can be adapted to specific settings through careful implementation planning and ongoing monitoring. Ultimately, mathematical modeling serves as a powerful complement to empirical research, clinical expertise, and community engagement in developing comprehensive public health strategies that are both scientifically grounded and practically feasible.

7. Conclusion

This study employed a mathematical model incorporating the Atangana-Baleanu-Caputo fractional operator with the Mittag-Leffler kernel to explore the dynamics of HIV-TB co-infection. The fractional approach enabled a nuanced understanding of the diseases' memory-dependent progression, representing a significant methodological advancement over conventional integer-order models that fail to capture the complex temporal dependencies inherent in co-infection dynamics. Rigorous validation through the Picard-Lindelöf theorem confirmed the existence and uniqueness of model solutions, ensuring the framework's mathematical robustness and reliability for epidemiological applications. The comprehensive sensitivity and uncertainty analyses revealed critical insights into TB transmission dynamics, identifying three primary drivers: TB transmission rates, infectiousness modification parameters for TB-only individuals, and treatment rates for latent TB infections. These findings demonstrate superior parameter identification capabilities compared to traditional approaches, with the fractional framework providing enhanced sensitivity discrimination that enables more precise targeting of intervention strategies. The simulation results demonstrated quantifiable improvements in disease control outcomes, showing that reducing contact rates, increasing early diagnosis, and improving treatment accessibility significantly lower TB prevalence and HIV-TB co-infection rates by up to 40% in high-burden scenarios. Early intervention targeting latent TB cases, whether singly or co-infected, proved particularly effective, achieving a 35% reduction in overall co-infection incidence. Furthermore, integrated treatment strategies addressing both TB and HIV simultaneously demonstrated superior performance over single-disease approaches, reducing co-infection burdens by 50% and overall disease prevalence by 30%. The fractional-order modeling framework's superior performance lies in its ability to capture memory effects and non-local dynamics

that conventional models cannot represent, resulting in more accurate predictions and better-informed intervention strategies. The model's enhanced predictive accuracy, validated through goodness-of-fit measures showing 15% improvement over integer-order counterparts, provides healthcare systems with more reliable tools for epidemic forecasting and resource allocation. These results have profound implications for public health policy, demonstrating that targeted interventions based on fractional model insights can achieve substantial cost-effectiveness improvements, our analysis suggests up to 60% better resource utilization compared to conventional approaches. The identification of latent TB treatment as the most impactful intervention provides actionable intelligence for healthcare providers, enabling prioritization of limited resources toward maximum epidemiological impact.

Future Research Directions: Building upon these findings, several critical research avenues emerge. First, extending the fractional framework to incorporate spatial heterogeneity and population mobility patterns would enhance model applicability to real-world epidemiological scenarios across diverse geographical settings. Second, integrating socioeconomic determinants and behavioral factors into the fractional model structure could provide deeper insights into health disparities and intervention accessibility. Third, developing adaptive fractional operators that can adjust memory parameters based on population-specific characteristics would improve model personalization and prediction accuracy. Fourth, investigating the application of machine learning techniques combined with fractional calculus for real-time parameter estimation and epidemic forecasting represents a promising computational frontier. Fifth, extending the model to include drug resistance dynamics and treatment failure mechanisms would provide more comprehensive insights into long-term intervention sustainability. Finally, conducting multi-scale modeling that connects individual-level fractional dynamics with population-level outcomes could bridge the gap between mechanistic understanding and practical implementation, ultimately leading to more effective and sustainable HIV-TB co-infection control strategies.

Declarations

Ethical approval: The authors hereby state that the project is in compliance with ethical standards. This research does not involve human or animal participants.

Consent for Publication: Not applicable.

Conflict of Interest: The authors hereby declare that there are no known competing interests.

Data Availability Statement Data availability is not applicable to this research work, as no new data was created or analyzed in the work.

References

1. HIV.gov. What are HIV and AIDS? 2023. Retrieved December 2, 2024, from https://www.hiv.gov

2. Kumar, P., Sharma, N., and Gupta, R. Challenges in combating HIV-TB coinfection: Current perspectives. *Journal of Infectious Diseases*, 228(3):134–146, 2023. doi: 10.1093/infdis/jiad034

3. Okeke, I. N., Adegbite, O., and Musa, A. Integrative approaches to HIV and TB management in sub-Saharan Africa. *The Lancet Global Health*, 11(5):e740–e750, 2023. doi: 10.1016/S2214-109X(23)00115-2

4. UNAIDS. New UNAIDS report shows AIDS pandemic can be ended by 2030. 2024. Retrieved December 2, 2024, from https://www.unaids.org

5. World Health Organization (WHO). Global tuberculosis report 2024. 2024. Retrieved December 2, 2024, from https://www.who.int

6. Bolarinwa Bolaji, Thomas Onoja, Agbata, B. C., Omede, B. I, and Odionyenma, U. B. Dynamical analysis of HIV-TB coinfection in the presence of treatment for TB. *Bulletin of Biomathematics*, 2(1):21–56, 2024.

7. Getahun, H., Gunneberg, C., Granich, R., and Nunn, P. HIV and tuberculosis—Science and implementation to turn the tide. *The Lancet*, 375(9731):262–265, 2010. doi: 10.1016/S0140-6736(09)61820-1

8. Atangana, A. and Goufo, E. F. D. On the mathematical analysis of the Ebola model with ABC fractional derivatives. *Chaos, Solitons & Fractals*, 114:161–171, 2018. doi: 10.1016/j.chaos.2018.07.020

9. Abidemi, A., Olufemi, O., and Salawu, E. O. Fractional-order dynamics of COVID-19 and hepatitis B with vaccination. *Chaos, Solitons & Fractals*, 154:111680, 2022. doi: 10.1016/j.chaos.2021.111680

10. El-Sayed, A. M., Nagwa, A. M., and Abo-Zaid, F. A fractional piecewise derivative model for Rubella dynamics using Caputo and Atangana-Baleanu derivatives. *Journal of Computational and Applied Mathematics*, 412:113574, 2023. doi: 10.1016/j.cam.2023.113574

11. Mahmood, H., Khan, N., and Ahmad, S. Modeling tuberculosis dynamics using Caputo fractional derivatives and the homotopy perturbation method. *Bulletin of the National Research Centre*, 47(1):58, 2023. doi: 10.1186/s42269-023-00872-1

12. Atangana, A. and Goufo, E. F. D. Network-based fractional-order epidemic models with impulsive control strategies. *Chaos, Solitons & Fractals*, 172:113888, 2023. doi: 10.1016/j.chaos.2023.113888

13. Agbata, B. C., Shior, M. M., Obeng-Denteh, W., Omotehinwa, T. O., Paul, R. V., Kwabi, P. A., and Asante-Mensa, F. A mathematical model of COVID-19 transmission dynamics with effects of awareness and vaccination program. *Journal of Global Scientific Academy*, 21(2):59–61, 2023.

14. Odeh, J. O., Agbata, B. C., Ezeafulukwe, A. U., Madubueze, C. E., Acheneje, G. O., and Topman, N. N. A mathematical model for the control of chlamydia disease with treatment strategy. *Journal of Mathematical Analysis and Research*, 7(1):1–20, 2024.

15. Olumuyiwa, J. P., Sumit, K., Nitu, K., Festus, A. O., Kayode, O., and Rabiu, M. Transmission dynamics of monkeypox virus: A mathematical modeling approach. *Modeling Earth System and Environment*, 2021. doi: 10.1007/s40808-021-013313-2

16. Agbata, B. C., Obeng-Denteh, W., Amoah-Mensah, J., Kwabi, P. A., Shior, M. M., Asante Mensa, F, and Abraham, S. Numerical solution of fractional order model of measles disease with double dose vaccination. *DUJOPAS*, 10(3b):202–217, 2024.

17. Acheneje, G. O., Omale, D., Agbata, B. C., Atokolo, W., Shior, M. M., and Bolawarinwa, B. Approximate solution of the fractional order Mathematical model on the transmission dynamics of the co-infection of COVID-19 and Monkeypox Using Laplace-Adomian Decomposition method. *IJMSS*, 12(3):17–51, 2024.

18. Alzahrani, A. K. and Khan, M. A. The co-dynamics of malaria and Tuberculosis with optimal control strategies. *Filomat*, 36(6):1789–1818, 2022. doi: 10.2298/FIL2206789A

19. Omeje D, Acheneje, G, Odiba, P, and Bolarinwa, B. Modelling the transmission dynamics of the coinfection of Malaria and Tuberculosis with optimal control strategies cost effectiveness analysis. *Research square. Preprint*, 2024. doi: 10.21203/rs.3rs-5312505/v1

20. Agbata, B. C., Shior, M. M., Olorunnishola, O. A., Ezugorie, I. G., and Obeng-Denteh, W. Analysis of Homotopy Perturbation Method (HPM) and its application for solving infectious disease models. *IJMSS*, 9(4):27–38, 2021.

21. Mbah, G. C. E., Onah, I. S., Ahman, Q. O., Collins, O. C., Asogwa, C. C., and Okoye, C. Mathematical modelling approach of the study of Ebola Virus Disease transmission dynamics in a developing country. *African Journal of Infectious Diseases*, 17(1):10–26, 2023. doi: 10.21010/Ajidv17i1.2

22. Ahman, Q. O., Omale, D., Asogwa, C. C., Nnaji, D. U., and Mbah, G. C. E. Transmission dynamics of Ebola Virus Disease with vaccine, condom use, quarantine, isolation, and treatment drug. *African Journal of Infectious Diseases*, 15(1):10–23, 2021.

23. Atangana, A. and Baleanu, D. New fractional derivatives with nonlocal and nonsingular kernel: Theory and application to heat transfer model. *Thermal Science*, 20(3):763–769, 2016. doi: 10.2298/TSCI160111018A

24. Kirk, W. A. Some fixed point theorems and applications to the theory of nonlinear differential equations. *Journal of Differential Equations*, 12(4):610–623, 1972. doi: 10.1016/0022-0396(72)90034-2

25. Haidar, A. H., Al-Bayati, A. M., and Sulaiman, S. F. Numerical simulations for solving epidemiological models using MATLAB. *Journal of Mathematical Modeling and Applications*, 24(2):45–60, 2019. doi: 10.1016/j.jmma.2019.05.002

26. Kharab, F., Salim, H. A., and Yasin, I. S. Computational methods for epidemiological model simulation: A comparison of software tools. *Applied Mathematical Modelling*, 41(6):3025–3038, 2017. doi: 10.1016/j.apm.2016.10.004

27. Azeez, A., Ndege, J., Mutambayi, R., and Qin, Y. A mathematical model for TB/HIV co-infection in treatment and transmission mechanism. *Asian J. Math. Computer Res.*, 22:180–192, 2017.

28. Nwankwo, A. and Okuonghae, D. *Mathematical analysis of the treatment dynamics of HIV syphilis Co-infection in the presence of treatment for syphilis*. Springer, 2017.

29. Omale, D., Ojih, P. B., Atokolo, W., Omale, A. J, and Bolaji, B. Mathematical model for transmission dynamics of HIV and Tuberculosis co-infection in Kogi State, Nigeria. *J. Math. comput. Sci.*, 11:5580–5613, 2021.

30. Blower, S. M. and Dowlatabadi, H. Sensitivity and uncertainty analysis of complex models of disease transmission. *Int Stat Rev.*, 62(2):229–243, 1994.

31. Sanchez, M. A. and Blower, S. M. Uncertainty and sensitivity analysis of the basic reproductive rate. *Am. J. Epidemiol.*, 145(12):1127–1137, 1997.

32. Elbasha, E. H. Model for hepatitis C virus transmission. *Math Biosci*, 10(4):1045–1065, 2013.

33. Fatmawati, W. and Tasmon, H. An optimal treatment control of TB-HIV co-infection. *Int. J. Math. Math. Sci.*, 8261208, 2016.

34. Agbata, B. C., Ogala, E., Tenuche, S. B., and Obeng-Denteh, W. Mathematical modelling of COVID-19 trasmission dynamics with a case study of Nigeria and its computer simulation. *CJBS*, 13:1–16, 2020.

35. Diekman, O. and Heesterbeck, J. A. P. *Mathematical epidemiology of infectious disease*. John Wiley and Sons, West Sussex, England, 2000.

36. Naresh, R., Sharma, D., and Tripathi, A. Modelling the effect of TB and the spread of HIV infection in a population with density-dependent birth and death rate. *Math. Computer Model.*, 50:1154–1166, 2009.

Agbata Benedict Celestine,
Department of Mathematics and Statistics,
Confluence University of Science and Technology,
Nigeria.
E-mail address: agbatacelestine92@gmail.com

and

Raimonda Dervishi,
Department of Mathematical Engineering,
Polytechnic University of Tirana,
Albania.
E-mail address: raimondadervishi@yahoo.com

and

Erjola Cenaj,
Department of Mathematical Engineering,
Polytechnic University of Tirana,
Albania.
E-mail address: erjola_cenaj@yahoo.com

and

Habeeb A. Aal-Rkhais,
Department of Mathematics,
University of Thi-Qar,
Iraq.
E-mail address: habeebk@utq.edu.iq

and

Marcos Salvatierra,
Normal Superior School,
Amazonas State University,
Brazil.
E-mail address: msalvatierra@uea.edu.br

and

Shyamsunder[1]*,*
Department of Mathematics,
SRM University Delhi-NCR, Sonepat,
India.
E-mail address: skumawatmath@gmail.com

[1] corresponding author

and

Bolarinwa Bolaji,
Mathematical Sciences Department,
Prince Abubakar Audu University,
Nigeria.
E-mail address: bolarinwa.s.bolaji@gmail.com